Nuclei containing an antinucleon

A. J. Baltz, C. B. Dover, and M. E. Sainio*
Brookhaven National Laboratory, Upton, New York 11973

A. Gal and G. Toker
Racah Institute of Physics, The Hebrew University, Jerusalem, Israel 91904
(Received 5 April 1985)

We have investigated the possibility that a nucleus containing a single antinucleon ($\bar{N}$) may exhibit some relatively long-lived excited states. Using $\bar{N}$ optical potentials consistent with the available data on $\bar{p}$-atom level shifts and/or low energy $\bar{p}$-nucleus scattering, and calculating the complex eigenvalues of the Schrödinger equation, we find that the annihilation widths of strongly bound (non-Coulomb) $\bar{N}$ states are generally large, as expected, of order $\Gamma \approx 50-100$ MeV. Some possible exceptions to this may occur when the $\bar{N}$ is bound to a light nuclear core which is not spin and isospin saturated. We obtain cross section estimates for the formation of $\bar{N}$ nuclei via the ($\bar{p}$,p) and ($\bar{p}$,n) reactions on nuclear targets with $A=3$, 4, and 16.

I. INTRODUCTION

The advent of the Low Energy Antiproton Ring (LEAR) facility at CERN has greatly expanded the possibilities for a detailed study of the interaction of antinucleons ($\bar{N}$) with nuclei. One eagerly awaits further data on elastic, inelastic, and charge exchange scattering and polarization on nuclear targets, as a means of extracting the systematics of the $\bar{N}$-nucleus optical potential [central, symmetry ($\boldsymbol{\tau}\cdot\mathbf{T}$), and spin-orbit parts, for instance]. Some intriguing first results on elastic and inelastic scattering are already available[1] from LEAR, which supplement data from KEK in Japan[2] and from Brookhaven.[3] The $\bar{N}$ may also be useful as a complement to more conventional probes of nuclear structure, because of its properties of extremely strong surface localization and the possible strong spin-isospin dependence of the $\bar{N}$ interaction with nucleons.

At this stage, it seems appropriate to pose a few qualitative questions regarding $\bar{N}$ interactions with nuclei. We explore the following ones:

(i) Could there exist any relatively long-lived excitations of an $\bar{N}$ in a nucleus, beyond the atomic states formed by the attractive $\bar{p}$-nucleus Coulomb potential?

(ii) What are the cross sections for producing $\bar{N}$ nuclei, for instance via the ($\bar{N}$,N) reaction?

At first glance, the answer to question (i) is negative, and indeed the first experimental results[4,5] on the ($\bar{p}$,p) reaction do not indicate narrow structure. The encounter of an $\bar{N}$ with a nucleon will typically lead to an *annihilation* process in which a burst of pions is produced (mean multiplicity ≈ 5). Using simple semiclassical arguments, the strong interaction width Γ associated with the process $N\bar{N} \rightarrow$ pions in the nucleus is or order 100 MeV. Hence, one does not anticipate a spectrum of narrow $\bar{N}$-nucleus states ($\Gamma < 10$ MeV, say), except of course for the $\bar{p}$-atomic states,[6-8] whose narrow width is due to the long range Coulomb attraction which serves to localize the $\bar{N}$ wave function well outside the radial domain of the short range annihilation potential. In the present paper, we indicate that there *may* be a few exceptions to this general expectation. Indeed, we find that for $\bar{N}$-nuclear bound states in finite nuclei the widths are generally large ($\Gamma > 50$ MeV), even for states of orbital angular momentum $L \neq 0$ within a few MeV of threshold, in rough agreement with the semiclassical estimate of Γ. However, in certain very light systems, where the nuclear core is not spin-isospin saturated, the real part of the $\bar{N}$-core potential can contain a contribution from one-pion exchange (OPE). The long-range piece can serve to localize the $\bar{N}$ wave function outside the region of strongest absorption, and hence reduce Γ below the semiclassical estimate Γ_0. More importantly, if the absorptive potential W is strongly spin and/or isospin dependent, Γ/Γ_0 can be suppressed for certain configurations in light systems.

To address question (ii), we have estimated formation cross sections for $\bar{N}$ nuclei via the ($\bar{N}$,N) reaction, using the distorted wave approximation. The experimental difficulty with the ($\bar{N}$,N) reaction, and also similar processes such as ($\bar{N}$,π), ($\bar{N}$,d), etc., is that significant backgrounds arise from $\bar{N}$ annihilation into pions, followed by π-induced emission of various secondary particles. A reaction leading to a high momentum exit particle is most easily distinguished from the background, which is concentrated at low momentum. However, a particle in the final state with large momentum corresponds to the formation of deeply bound $\bar{N}$-nucleus states, which are expected to be very broad. Thus one does not expect sharp structures in the high momentum part of the exit particle, but rather a smooth tail which may rise above the background predicted by simple cascade calculations.

The paper is organized as follows: In Sec. II, we discuss the choice of the $\bar{N}$-nucleus optical potential $V_{\rm opt}(r)$. The available $\bar{p}$-atom and low energy $\bar{p}$ scattering data only determine the potential in a narrow spatial region around a strong absorption radius (typically two to three surface diffusenesses outside the nuclear radius R). The bound state $\bar{N}$ spectrum, on the other hand, also depends

sensitively on the interior region of the potential, which is largely undetermined.

In Sec. III, we discuss several typical spectra of $\bar{N}$ bound and continuum states. Deeply bound states arise only when $V_{opt}(r)$ is strongly attractive in the nuclear interior, a situation not favored by recent phenomenological analyses,[1-3] which lead to attractive but rather shallow real potentials.

The most natural way of producting $\bar{N}$ nuclei is through the ($\bar{N}$,N) reaction. In Sec. IV, some sample cross sections are given for the ($\bar{p}$,p) reaction on an ^{16}O target. For the broad $\bar{p}$ bound states, we find $d\sigma/d\Omega$ to be as large as 0.5 mb/sr, while the cross sections to $\bar{p}$-atomic states are typically three orders of magnitude smaller. The calculations were done in the distorted wave Born approximation (DWBA), with phenomenological $\bar{p}$ and p potentials consistent with those used for the bound state calculation. The transition operator is constructed in zero range approximation from the observed $\bar{p}p \to \bar{p}p$ differential cross section at 180°.

In Sec. V, we investigate some special features which may prevail for light $\bar{N}$-nucleus systems. Since the $N\bar{N}$ interaction is spin-isospin dependent, quite strongly in some models, the binding energies and widths of $\bar{N}$ states depend on the spin S_c and isospin I_c of the nuclear core. These effects are relatively more important when the number of core nucleons A is small. In particular models, notably that of the Paris group,[9] the imaginary part of the $\bar{N}N$ potential is much stronger for the spin singlet state than for the spin triplet. If this is true, the widths of $\bar{N}$ states may exhibit an interesting spin *selectivity*, analogous to that which occurs[10] in the Σ hypernucleus ${}^{6}_{\Sigma}H$.

We argue that if such states are narrower than about 25 MeV, they should be observable at LEAR via a study of the $^3He(\bar{p},p)X$ or $^4He(\bar{p},n)X$ reactions at energies of 100–200 MeV. The most likely candidate for a narrow three- or four-body state is the $\bar{N}NN$ system with spin $S_x=\frac{3}{2}$ and isospin $I_x=\frac{1}{2}$. A brief summary is given in Sec. VI.

II. THE $\bar{N}$ OPTICAL POTENTIAL

Our knowledge of the antinucleon-nucleus optical potential $V_{opt}(r)$ is rather limited. Several analyses[11-14] of the complex level shifts in $\bar{p}$ atoms and low-energy $\bar{p}$-nucleus scattering[1-3,15,16] have been performed. Often $V_{opt}(r)$ is parametrized in terms of a Woods-Saxon potential

$$V_{opt}(r) = -V_0\left[1+\exp\left(\frac{r-R_v}{a_v}\right)\right]^{-1} - iW_0\left[1+\exp\left(\frac{r-R_w}{a_w}\right)\right]^{-1} \quad (2.1)$$

with $R_v=r_{0v}A^{1/3}$ and $R_w=r_{0w}A^{1/3}$, A being the number of nucleons in the core. The parameters of three such potentials are collected in Table I. The potential of Barnes *et al.*[11] cited in the table represents a best fit to the level shift in the $\bar{p}+{}^{16}O$ system. The other two potentials[1,16] are obtained from fits to the $\bar{p}+{}^{12}C$ elastic scattering data at $E=46$ MeV, but they are also consistent with the $\bar{p}+{}^{12}C$ atomic level shift.

The potentials fitted to low energy $\bar{p}$ scattering data have a shallower real part than the older models[11-13] based on $\bar{p}$-atom data. A recent combined analysis of low energy scattering and $\bar{p}$-atom data by Batty *et al.*[15] favors the shallower potentials, and does not require the potentials to be energy dependent, at least in the regime below 50 MeV. Note, however, that a number of theoretical calculations[17-19] indicate that V_{opt} should be energy dependent, with a change of sign of the real part at some finite energy, roughly between 100 and 200 MeV. For our bound state calculations, such an energy dependence is largely irrelevant, but for the study of unstable bound states (UBS's) in the continuum, it introduces an additional uncertainty in our calculations.

The $\bar{p}$-atom level shifts and also low energy scattering are only sensitive to $V_{opt}(r)$ in the far surface region. For instance, Garreta *et al.*[1] obtain a whole family of equivalent fits to the elastic $\bar{p}$ data characterized by the approximate constancy of $\mathrm{Re}V_{opt}(r)/\mathrm{Im}V_{opt}(r)$ near a strong absorption radius $R_{abs}\approx 3.6$ fm for $\bar{p}+{}^{12}C$, well outside the half-radius $R_v\approx 2.5$ fm. Using a Fourier-Bessel expansion of the $\bar{p}$ potential, Batty *et al.*[15] have shown how the uncertainties in the $\bar{p}$ well depths V_0 and W_0 become very large as one penetrates the nuclear interior.

For the problem we are interested in, namely $\bar{p}$-nucleus bound states, the internal part of $V_{opt}(r)$ plays a more important role. If $\mathrm{Re}V_{opt}(r)$ is strongly attractive in the interior, a number of $\bar{p}$-nucleus bound states with large binding energy E_B can be formed. Even though we expect these objects to be very broad, they still have an experimental consequence, namely the appearance of protons from the ($\bar{p}$,p) reaction with momenta k considerably higher than the $\bar{p}$ beam momentum k_L. In this regime ($k>k_L$), the background spectrum of protons, due to $\bar{p}$ annihilation followed by pion knockout of secondary nucleons, is expected to be small. Even in the absence of narrow internal $\bar{p}$ states, the momentum spectrum of the exit proton might still contain some rough information on the $\bar{p}$ well depth for $r<R_v$.

The potentials of Table I are appropriate for a $\bar{p}$ interacting with a spin-isospin saturated ($S_c=0$, $I_c=0$) nuclear core. The size of the spin and isospin dependent terms in the $\bar{p}$-nucleus potential are essentially unknown, although the comparative analysis of Poth *et al.*[13] for

TABLE I. Antinucleon optical model parameters.

Reference	V_0 (MeV)	W_0 (MeV)	r_{0v} (fm)	r_{0w} (fm)	a_v (fm)	a_w (fm)
Barnes *et al* (Ref. 11)	167.7	79.4	1.032	1.032	0.5	0.5
Friedman (Ref. 16)	47.97	65.64	1.0234	1.0234	0.552	0.682
Garetta *et al.* (Ref. 1)	25	61	1.167	1.195	0.608	0.508

$\bar{p} + {}^{16}O$ and $\bar{p} + {}^{18}O$ atoms indicates a sizable isospin dependence for $V_{opt}(r)$, i.e., a Lane potential proportional to $\tau_{\bar{N}} \cdot \mathbf{I}_c$. Such spin and isospin dependent terms in both the real and imaginary parts of $V_{opt}(r)$ are expected theoretically, since the two-body $N\bar{N}$ interaction exhibits a rather strong spin-isospin dependence. In Sec. V, we focus on the problem of a $\bar{p}$ interacting with an unsaturated light (two or three nucleons) core. Here, the widths of particular $\bar{p}$ bound states can be reduced by the spin-isospin dependence of $V_{opt}(r)$. This offers the best possibility for observing relatively narrow (non-Coulomb) $\bar{p}$ bound states.

III. THE SPECTRUM OF BOUND AND CONTINUUM $\bar{p}$-NUCLEUS STATES

In this section, we show some typical results for the bound and continuum (UBS) states of the $\bar{p} + {}^{11}B$ ($^{12}_{\bar{p}}Be$) and $\bar{p} + {}^{15}N$ ($^{16}_{\bar{p}}C$) systems. These could be populated in the ^{12}C $(\bar{p},p)^{12}_{\bar{p}}Be$ and $^{16}O(\bar{p},p)^{16}_{\bar{p}}C$ reactions, respectively. Our preliminary results were reported in Ref. 20; other examples of bound state spectra are given in Refs. 21 and 22. Before proceeding, it is useful to make some qualitative arguments regarding the scale of the widths Γ of $\bar{N}$-nucleus states. If the binding energy E_B is large (deep real potential), the $\bar{N}$ wave function is localized inside the well, and one obtains the limiting value $\Gamma \approx 2W_0$. For any realistic W_0, this gives $\Gamma \gtrsim 100$ MeV. In practice, the calculated widths are somewhat less than $2W_0$ since some of the wave function leaks out of the well. However, we do not obtain narrow widths ($\Gamma < 20$ MeV, say), even if the binding energy is only a few MeV. An exception is the Coulomb-type bound states, for which the wave function is localized far from the nucleus.

In Table II, we give the energy shifts ΔE and widths Γ of $\bar{p} + {}^{15}N$ states with the $\bar{p}$ in an s- or p-wave orbit around the ^{15}N core. The $\bar{p}$ potential of Barnes *et al.*[11] from Table I was used. We solved the Schrödinger equation for the complex eigenvalues $E_B - i\Gamma/2$, using a modified version of the program EXOTIC due to Koch and Sternheim.[23] The shifts ΔE are taken with respect to the point Coulomb binding energies.

The spectrum of Table II is typical for a model with a deep real $\bar{p}$ potential in the nuclear interior. Several deeply bound states are produced, but these are broad ($\Gamma \approx 100$ MeV). The s ($n=2$) state is unstable bound state (UBS) in the continuum, also quite broad in this case. The s ($n=3$) and p ($n=2$) states are the shifted $\bar{p}$-atomic states, which evolve continuously from the nodeless $1s$ and $2p$ eigenstates of the Coulomb potential as the strong interaction is turned on. Note that these shifted "atomic" states acquire additional radial nodes, in order to remain orthogonal to the "nuclear" states of the same orbital angular momentum L. These nodes occur in the nuclear interior, and do not disturb the essential localization property of the atomic states at distances well outside the nucleus. The large rms radii of the atomic states ensures that their widths Γ are small. Note that the strong interaction shift ΔE is repulsive ($\Delta E > 0$) for these states.

TABLE II. Energy shifts ΔE and widths Γ for s- and p-wave $\bar{p} + {}^{15}N$ states calculated using the parameters of Barnes *et al.* (Ref. 11) from Table I.

$\bar{p}$ orbit	ΔE (MeV)	Γ (MeV)
s ($n=0$)	−116	116
s ($n=1$)	−48	94
s ($n=2$)	+12	45
s ($n=3$)	+0.7	0.15
p ($n=0$)	−86	108
p ($n=1$)	−17	77
p ($n=2$)	+0.019	0.028

The s- and p-wave $\bar{p} + {}^{15}N$ atomic states cannot be seen directly in a γ-ray cascade, since strong absorption already dominates $E1$ γ-ray emission in the d state.[11–13] Nevertheless, these levels are of considerable interest, since they contain additional information on the radial dependence of $V_{opt}(r)$. Cross section estimates for their formation in $(\bar{p},p)$ reactions were first presented in Ref. 20. Their importance has also been emphasized by Gibbs and Kaufmann,[8] who found a case where the $(\bar{p},p)$ formation cross section may be large enough to be observed above the background. We return to this question in Sec. IV.

In Table III, we give E_B and Γ for the $\bar{p} + {}^{11}B$ nuclear states, using the potentials of Garreta *et al.*[1] and Friedman[16] from Table I. A folded Coulomb potential is included in the calculation. These potentials, which fit low energy ($E=46$ MeV) $\bar{p} + {}^{12}C$ elastic scattering, have rather shallow real parts, so only the nodeless s ($n=0$) state is bound. The other states in Table III are normalizable unstable bound states[24] (UBS's) embedded in the $\bar{p}$ continuum. Because of their greater degree of localization at the surface, the UBS's are narrower than the states with $E_B < 0$. The widths of these UBS's are to a first approximation independent of the depth of the real potential. Although one can produce narrow UBS's in $^{12}_{\bar{p}}Be$ ($\Gamma < 20$ MeV or so), for instance an f ($n=0$) state, by modest changes of V_0 and W_0, these always lie rather high in the continuum ($E_B > 40$ MeV), so the results become very model dependent. Another problem is that formation of the UBS's in the $(\bar{p},p)$ reaction would correspond to protons with momentum $k < k_L$, where the background from annihilation is highest. One might note from Table III the approximately "harmonic" level ordering of the UBS's, i.e., the s ($n=1$) and d ($n=0$) states are almost degenerate and the s ($n=0$), p ($n=0$), and d ($n=0$) states form an approximately equidistant sequence. One can

TABLE III. Binding energies E_B and widths Γ for $\bar{p} + {}^{11}B$ states calculated using the parameters of Garreta *et al.* (Ref. 1) or Friedman (Ref. 16) (in parentheses) from Table I.

$\bar{p}$ orbit	E_B (MeV)	Γ (MeV)
s ($n=0$)	−2(−17)	95(91)
s ($n=1$)	40(25)	21(26)
p ($n=0$)	18(6)	69(66)
d ($n=0$)	39(27)	36(35)

TABLE IV. Variation of binding energy shift ΔE and width Γ of the p ($n=0$) state of $\bar{p}+{}^{15}N$ with W_0 for fixed $V_0=166$ MeV.

W_0 (MeV)	ΔE (MeV)	Γ (MeV)
0	−84.8	0
35	−84.9	47
61	−85.2	83
79	−85.5	108

deduce an equivalent harmonic oscillator spacing $\hbar\omega \approx 20$ MeV from Table III, and observe that the calculated s ($n=0$) level lies about $\frac{3}{2}\hbar\omega$ in energy above the bottom of the potential well, as it should.

It is instructive to see how ΔE and Γ evolve as we change the well depths V_0 and W_0. Two typical examples are shown in Tables IV and V. If one keeps V_0 fixed and increases W_0 from zero to its full phenomenological value, Γ increases linearly with W_0 and ΔE remains essentially fixed (for a deeply bound state). This behavior is shown in Table IV. On the other hand, if one keeps W_0 fixed and reduces V_0, the binding of the $\bar{p}$ state decreases but *its width is essentially independent of* V_0, as shown in Table V. *Even as the nuclear state passes through zero binding, its width remains large,* contrary to what one might naively expect from perturbation theory. This is because the imaginary part of $V_{\rm opt}(r)$ serves to keep a considerable part of the wave function localized in the nuclear interior, even when the attraction from the real part is weak. In perturbation theory, on the other hand, one writes

$$\frac{\Gamma}{2} = -\int d^3r \,|\psi(r)|^2 \mathrm{Im} V_{\rm opt}(r) \,, \tag{3.1}$$

where $\psi(r)$ is the $\bar{N}$ wave generated by the *real* potential alone. In this case, as $E_B \to 0$, the wave function $\psi(r)$ is pushed out of the nucleus, and Γ becomes small. In a realistic situation with strong absorption, as here, Eq. (3.1) is valid only if ψ is generated by the full complex potential, for the normalization $\int |\psi|^2 d^3r = 1$.

In summary, our calculations indicate, as expected, that $\bar{N}$ nuclear states are broad ($\Gamma > 50$ MeV), even if they are weakly bound. Here, we have assumed the average absorptive potential appropriate to a spin-isospin saturated core. We investigate the possibility of "quenching" of Γ for unsaturated cores in Sec. V.

TABLE V. Variation of ΔE and Γ of the p ($n=1$) state[a] of $\bar{p}+{}^{16}O$ with V_0 for fixed $W_0=79$ MeV.

V_0 (MeV)	ΔE (MeV)	Γ (MeV)
166	−50	61.4
131	−29	63.0
96	−9	62.3
82	−0.9	60.7
81	0.08	60.4
79	1.1	60.1
56	15	53.7

[a]An attractive real term proportional to the second derivative of the Woods-Saxon form of Eq. (2.1) has been added here to the potential of Barnes *et al.* (Ref. 11) from Table I.

IV. PRODUCTION OF $\bar{N}$ NUCLEI IN THE ($\bar{N}$,N) REACTION

In this section, we present some estimates of the production cross sections for $\bar{p}$ nuclei in the ($\bar{p}$,p) reaction on ^{16}O. We have used the usual distorted wave Born approximation (DWBA) for our estimates.[25] In DWBA, the ($\bar{p}$,p) cross section in the laboratory system is given by

$$\left[\frac{d\sigma}{d\Omega}\right]^{fi} = \alpha_{fi}\left[\frac{d\sigma}{d\Omega}\right]^{\bar{p}p\to p\bar{p}}_{L,0^\circ} |F_{fi}(q)|^2 \,, \tag{4.1}$$

where α_{fi} is a spin-isospin coefficient, $0 \le \alpha_{fi} \le 1$, $\mathbf{q}=\mathbf{k}-\mathbf{k}'$ is the momentum transfer and $F_{fi}(q)$ is the nuclear form factor. In a simplified form which neglects recoil corrections,[25] we have

$$F_{fi}(q) = \int d^3r\, \psi_{\rm p}^{(-)*}(\mathbf{k}',\mathbf{r})\rho_{fi}(\mathbf{r})\psi_{\bar{\rm p}}^{(+)}(\mathbf{k},\mathbf{r}) \,, \tag{4.2}$$

where $\psi_{\rm p}^{(-)}$ is the appropriate distorted wave of the proton, $\psi_{\bar{\rm p}}^{(+)}$ is the distorted wave for the antiproton, and ρ_{fi} is the transition density defined by

$$\rho_{fi}(\mathbf{r}) = \langle f | \sum_{\alpha\beta} \tilde{\psi}^*_\beta(\mathbf{r})\psi_\alpha(\mathbf{r}) a^\dagger_{\bar{\rm p}}(\beta) a_{\rm p}(\alpha) | i \rangle \,. \tag{4.3}$$

Here ψ_α and ψ_β are bound state wave functions for the p and $\bar{p}$, respectively. The wave function $\tilde{\psi}_\beta$ is obtained by reversing the sign of $W(r)$, but $\tilde{\psi}^*_\beta$ essentially coincides with ψ_β. We consider transitions from a single proton bound state $\alpha = i(n_i,l_i,j_i)$ to a $\bar{p}$ bound state $\beta = f(n_f,l_f,j_f)$. The complex bound state $\bar{p}$ wave functions are normalized according to [22] $\int d^3r\, \psi_f^2(\mathbf{r}) = 1$ rather than $\int d^3r\, |\psi_f(\mathbf{r})|^2 = 1$. Note that the former normalization embodies *two* conditions, one being the orthogonality of the real and imaginary parts of ψ_f; this causes the number of radial nodes of Re ψ_f and Im ψ_f to differ by one. In this section, we use the alternative notation nl_j for nuclear states, where n is one greater than the number of inner nodes of the real part of the radial wave function. This is the equivalent of the notation $l(n-1)$ used in Sec. III. For these calculations, we have used the same $\bar{p}$ optical potential $V_{\rm opt}(r)$, from Barnes *et al.*[11] as per Table II, to generate both $\psi_{\bar{\rm p}}^{(+)}$ and ψ_f, thereby ignoring the (not yet established) energy dependence of $V_{\rm opt}$.

To generate ψ_i, we use a real Woods-Saxon potential (no spin-orbit term) with $r_{0v}=1.15$ fm, $a_v=0.63$ fm and adjust V_0 to reproduce the observed binding energy of the proton orbit. Here, we show results only for the orbit $i=\{1p_{3/2}\}$. Transitions involving the deeply bound $1s_{1/2}$ orbit are more strongly suppressed by the effect of initial state absorption, whereas transitions involving the $1p_{1/2}$ proton orbit are comparable to those we illustrate here.

The outgoing proton distorted waves $\psi_{\rm p}^{(-)}$ are obtained by solving the Schrödinger equation with a proton optical potential $V^{\rm p}_{\rm opt}(r)$ which has been adjusted to fit $p+{}^{16}O$ elastic scattering data[26] at $E_{\rm p}=150$ MeV. This potential has Woods-Saxon parameters $V_0=18.7$ MeV, $W_0=10.42$ MeV, $r_{0v}=1.13$ fm, $a_{0v}=0.72$ fm, $r_{0w}=1.18$ fm,

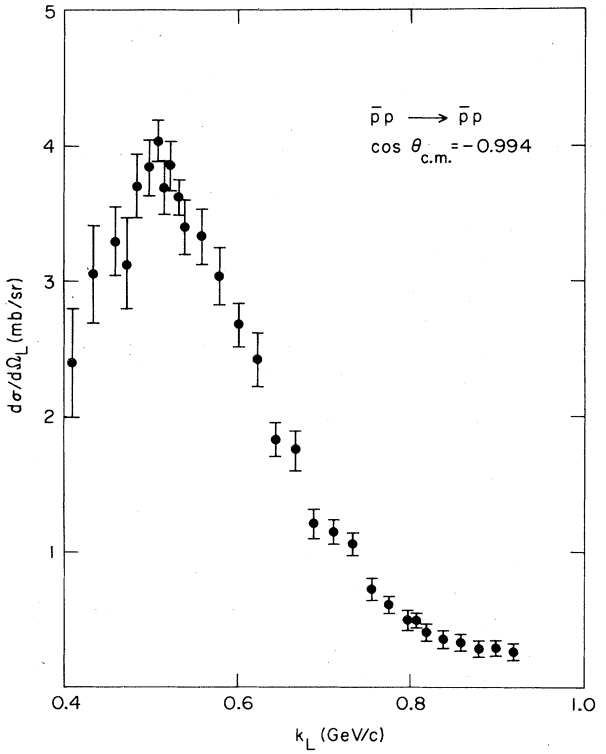

FIG. 1. Laboratory differential cross section $d\sigma/d\Omega_L$ for $\bar{p}p$ backward elastic scattering as a function of antiproton laboratory momentum k_L. The points and error bars were obtained using the approximate formula $d\sigma/d\Omega_L \approx 4 d\sigma/d\Omega_{c.m.}$, valid near $\cos\theta_{c.m.} = -1$, and the data for $d\sigma/d\Omega_{c.m.}$ of Alston-Garnjost *et al.* (Ref. 27).

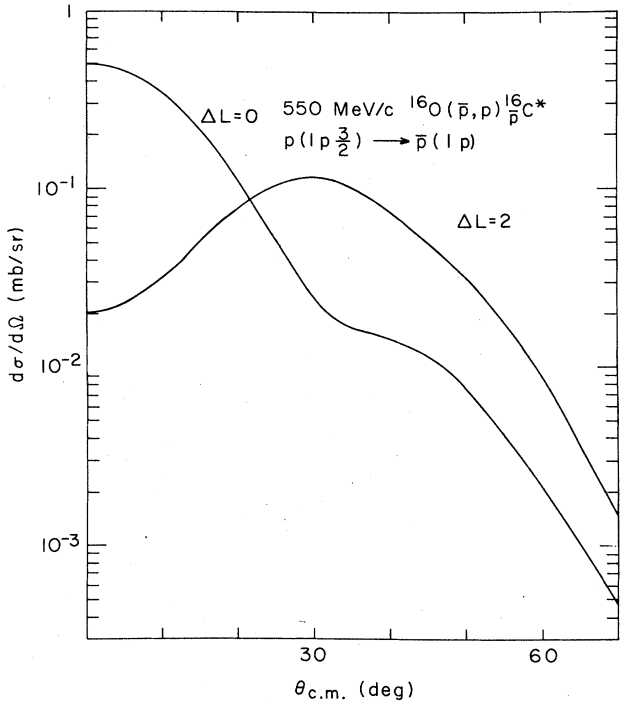

FIG. 2. Predicted angular distribution $d\sigma/d\Omega$ (c.m. system) for the $^{16}O(\bar{p},p)^{16}_{\bar{p}}C$ reaction at $k_L = 550$ MeV/c, corresponding to the $1p_{3/2} \rightarrow 1p_j$ single particle $p \rightarrow \bar{p}$ transition. The curves labeled by orbital angular momentum transfers $\Delta L = 0$, 2 refer to the summed population of final states of the $^{16}_{\bar{p}}C$ system with spin parity $J^\pi = 0^- - 3^-$ arising from the $(1p_{3/2}^{-1} \times 1p_j)$ proton hole-antiproton particle configuration (4.4). The DWBA calculation was performed for a Q value of 68 MeV, corresponding to the centroid of the broad $1p$ bound state of the $\bar{p}$.

$a_{0w} = 0.85$ fm for the central part, and $V_0^{so} = 3.52$ MeV, $W_0^{so} = -2.11$ MeV, $r_0^{so} = 0.93$ fm, $a^{so} = 0.5$ fm for the Thomas spin-orbit component. We assume that the potential for $p + {}^{16}O$ is also representative of the distortion effect for the final state $p + {}^{16}_{\bar{p}}C$. In any case, the choice of this potential is not crucial, since the reduction of cross sections from their limits in plane wave approximation (PWA) is due mainly to initial state absorption.

The other ingredient in Eq. (4.1) is the forward $\bar{p}p \rightarrow p\bar{p}$ cross section, which, loosely speaking, is identified with the 90° $\bar{p}p \rightarrow \bar{p}p$ elastic cross section in the laboratory frame (corresponding to the *backward* elastic $\bar{p}p$ cross section in the two-body center of mass frame). The most reliable measurements of large angle elastic scattering are due to Alston-Garnjost *et al.*[27] The behavior of the large angle *laboratory* cross section (actually $\theta_{c.m.} = 174°$) is shown in Fig. 1, as a function of k_L. *A priori*, one would like to choose a larger incident $\bar{p}$ momentum, in order that the final state proton is also more energetic, and hence less likely to be confused with a "background" proton due to $\bar{p}$ annihilation. However, as seen from Fig. 1, $(d\sigma/d\Omega)_L$ peaks at about $k_L = 510$ MeV/c and drops rapidly above 550 MeV/c although a second peak of diffractive character at higher momentum is not ruled out experimentally. In our calculations, we have taken $k_L = 550$ MeV/c ($E_{\bar{p}} = 150$ MeV) and used the value $(d\sigma/d\Omega)_L = 3.37$ mb/sr.

Our calculational procedure is as follows: we first construct the wave function $\tilde{\psi}_f^*(\mathbf{r})$ for the bound $\bar{p}$ from the modified code[23] EXOTIC and then, after obtaining $\psi_i(\mathbf{r})$ from a standard Woods-Saxon bound state search routine, we form the complex product $\tilde{\psi}_f^*(\mathbf{r})\psi_i(\mathbf{r})$ to which the transition density (4.3) reduces for a single particle transition. This is read in as a numerical form factor to the standard distorted wave program[25] CHUCK, which computes the differential cross sections in DWBA.

Some typical results for $1p_{3/2} \rightarrow np_j$ transitions are shown in Figs. 2–4. The final states considered in $^{16}_{\bar{p}}C$ are assumed to be of pure particle-hole structure

$$(1p_{3/2}^{-1} \times np_j)J^\pi, \quad j = \tfrac{1}{2}, \tfrac{3}{2}, \tag{4.4}$$

with respect to a closed ^{16}O p shell. In Eq. (4.4), we have $J^\pi = 0^-$, 1^-, 2^-, and 3^-. It is inconceivable that these states are separable from each other in the $(\bar{p},p)$ reaction: for the states of *nuclear* type ($n = 0,1$) this is due to the large width of each of these, while for the atomic type ($n = 2$) this holds due to the (~ 1 MeV) resolution of the final protons. For this reason, we have plotted in these figures the total $\Delta L = 0$ and $\Delta L = 2$ cross sections, where the $\Delta L = 0$ transition populates the 0^- state ($\Delta S = 0$) and

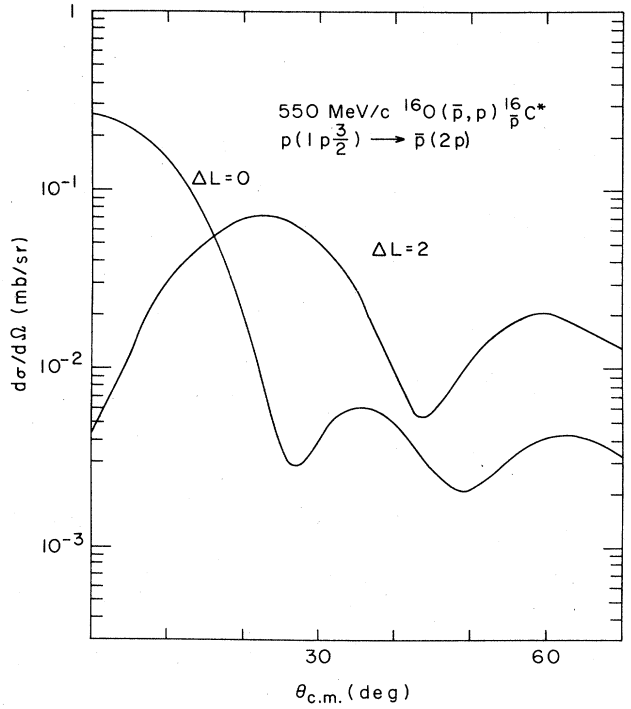

FIG. 3. Differential cross section $d\sigma/d\Omega$ for the $1p_{3/2} \rightarrow 2p_j$ single particle transition in the $^{16}O(\bar{p},p)^{16}_{\bar{p}}C$ reaction, calculated at the central value $Q=1$ MeV for the broad $2p$ state of the $\bar{p}$. The curves are labeled as in Fig. 2.

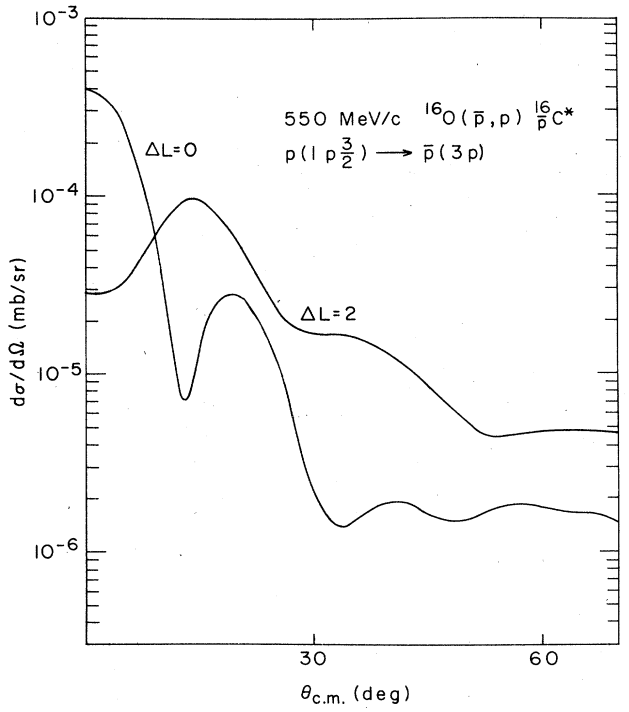

FIG. 4. Differential cross section for the $1p_{3/2} \rightarrow 3p_j$ transition in the $^{16}O(\bar{p},p)^{16}_{\bar{p}}C$ reaction at 550 MeV/c. The cross section for the narrow "quasiatomic" $3p$ state is seen to be about three orders of magnitude smaller than those shown in Figs. 2 and 3 for strongly bound $\bar{p}$ states.

the 1^- states ($\Delta S=1$), and the $\Delta L=2$ transition populates the 1^- states ($\Delta S=1$), the 2^- states ($\Delta S=0,1$), and the 3^- state ($\Delta S=1$). With this effective summation over ΔS, the coefficient α_{fi} in Eq. (4.1) becomes equal to one. The values of α_{fi} before summation may be deduced from Table X in the Appendix. In these calculations, we have evaluated the cross section at a Q value corresponding to the centroid of the broad $\bar{p}$ bound states. The Q value is defined in the usual way in terms of the initial and final state masses:

$$Q_0 = m(^{16}O) - m(^{15}N) - m_p - E_B(\bar{p}) ,$$

where the binding energy $E_B(\bar{p})$ is negative for a bound $\bar{p}$ state. Equivalently, we have $Q_0 = E_B(p) - E_B(\bar{p})$.

Figures 2 and 3 correspond to the formation of strongly bound $\bar{p}$-nuclear states. We see that there is only a relatively small penalty (a factor of 2) for changing the number of radial nodes by one. This is due to the very strong effects of $\bar{p}$ absorption for such deeply bound states (reduction of more than an order of magnitude relative to PWA), which reduces the sensitivity to the presence of nodes in the $\bar{p}$ radial wave function in the nuclear interior.

As usual, the coherent $\Delta L=0$ transitions are forward peaked while the $\Delta L=2$ transitions are negligible at small angles. Note that the peak value (at finite angles) of the $\Delta L=2$ cross sections is about a factor of 5 less than that for $\Delta L=0$.

In Figure 4, we display the $(\bar{p},p)$ cross sections for the production of *atomic states* of structure (4.4). For the case we have chosen, $^{16}O(\bar{p},p)^{16}_{\bar{p}}C$, these cross sections are three orders of magnitude smaller than those for strongly bound states. Our case is unfavorable, however, for atomic formation, since there is very little radial overlap between the $\bar{p}$-atomic wave function and the rather strongly bound $p_{3/2}$ proton in ^{16}O. In an interesting paper, Gibbs and Kaufmann[8] have looked for cases where this radial overlap is maximized: for the example of $^{31}P(\bar{p},p)$, they obtain an atomic cross section more than an order of magnitude larger than we get for the $^{16}O(\bar{p},p)$ reaction.

In Figs. 2–4, we used the central value $Q=Q_0$ to evaluate $d\sigma/d\Omega$. This may appear questionable, since the DWBA cross sections depend on Q through the dependence of the exit proton energy $E_p = E_{\bar{p}} + Q$, and a broad $\bar{p}$-state would sample a sizable range of Q values. To check this point, we have calculated $d\sigma/d\Omega$ for a set of Q values determined by the width of the $\bar{p}$ state ($Q=Q_0-\Gamma$, $Q_0-\Gamma/2$, Q_0, $Q_0+\Gamma/2$, $Q_0+\Gamma$) and averaged the results over a normalized distribution $f(E)$ of the form

$$f(Q) = \frac{1}{2\pi} \frac{\Gamma}{(Q-Q_0)^2 + (\Gamma/2)^2} . \tag{4.5}$$

For the $1p_{3/2} \rightarrow np_j$ transitions, we find average values (in mb/sr)

$$\left\langle \frac{d\sigma}{d\Omega}(0^\circ) \right\rangle = \int f(Q) \frac{d\sigma}{d\Omega}(Q) dQ = \begin{cases} 0.47 \text{ for } 1p_{3/2} \rightarrow 1p_j \\ 0.25 \text{ for } 1p_{3/2} \rightarrow 2p_j \end{cases} \tag{4.6}$$

while the cross sections evaluated at $Q=Q_0$ are (in mb/sr)

$$\frac{d\sigma}{d\Omega}(0^\circ)=\begin{cases}0.50 \text{ for } 1p_{3/2}\rightarrow 1p_j \\ 0.26 \text{ for } 1p_{3/2}\rightarrow 2p_j\end{cases}. \tag{4.7}$$

Thus, the effect of a large width on $d\sigma/d\Omega$ is negligible. However, the effect of Q dependence has a more pronounced influence on the *shape of the proton energy spectrum* in the $(\bar{p},p)$ reaction. For the excitation function, we have

$$\frac{d^2\sigma}{d\Omega\, dE_p}=\frac{\Gamma/2\pi}{(E_p-E_{\bar{p}}-Q_0)^2+(\Gamma/2)^2}\frac{d\sigma}{d\Omega}(Q), \tag{4.8}$$

where $E_{\bar{p}}$ is the bombarding energy. The energy spectrum $d^2\sigma/d\Omega\, dE_p$ at $\theta=0^\circ$ is shown in Fig. 5 for the $1p_{3/2}\rightarrow 2p_j$ transitions, using Eq. (4.8). The dashed curve represents the approximation used by Heiselberg *et al.*,[28] who replaced $d\sigma/d\Omega(Q)$ by $d\sigma/d\Omega(Q_0)$ in Eq. (4.8), thereby obtaining a pure Lorentzian line shape. This is seen to be a rather poor approximation to the line shape, which is considerably skewed towards higher Q by the factor $d\sigma/d\Omega(Q)$, although the energy-integrated cross section remains essentially the same, as per Eqs. (4.6) and (4.7).

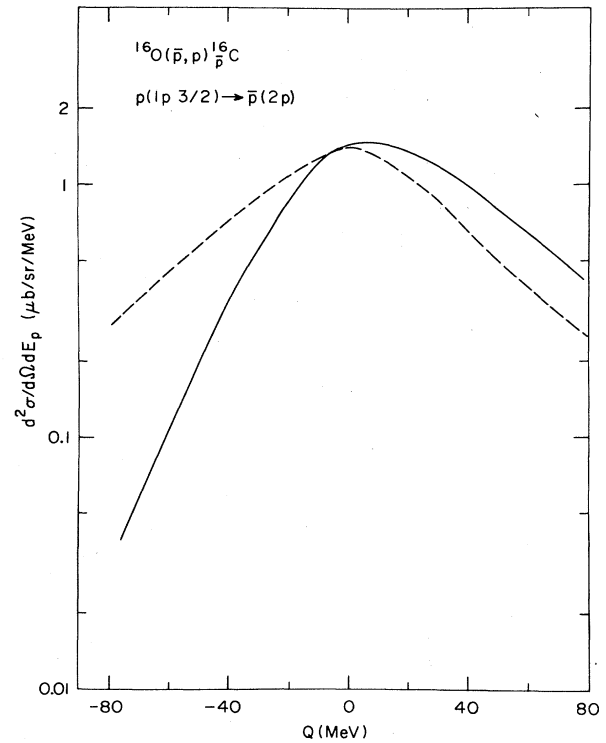

FIG. 5. The double differential cross section $d^2\sigma/d\Omega\, dE_p$ at $\theta=0^\circ$ for the $1p_{3/2}\rightarrow 2p_j$ transition in the $^{16}O(\bar{p},p)^{16}_{\bar{p}}C$ reaction at 550 MeV/c, as a function of Q (or, equivalently, the exit proton's kinetic energy $E_p=E_{\bar{p}}+Q$). The solid curve corresponds to a set of DWBA calculations performed at different Q values and then weighted according to the normalized distribution $f(Q)$ of Eq. (4.5) for the broad $\bar{p}$ state, as per Eq. (4.8). The dashed curve corresponds to the approximation adopted in Ref. 28, where $d\sigma/d\Omega(Q)$ in Eq. (4.8) is replaced by $d\sigma/d\Omega(Q_0)$.

The peak cross sections of $d^2\sigma/d\Omega\, dE_p$ in Fig. 5 are of order 1—2 μb/sr/MeV, *two orders of magnitude smaller than those shown in Fig. 1 of Heiselberg et al.*[28] for the $^{16}O(\bar{p},p)^{16}_{\bar{p}}C$ reaction. There are several reasons for this large discrepancy. Firstly, these authors[28] use the PWA, which overestimates the cross section by more than a factor of 10 for nuclear $\bar{p}$ states. Even for the $^{31}P(\bar{p},p)$ transition to $\bar{p}$-atomic states considered by Gibbs and Kaufmann,[8] absorptive effects still diminish the cross section by a factor of 2. Secondly, all single particle transitions from $s_{1/2}$, $p_{1/2}$, or $p_{3/2}$ proton states to $s_{1/2}$, $p_{1/2}$, and $p_{3/2}$ (and perhaps other) $\bar{p}$-bound states are summed in PWA in Ref. 28, whereas we have shown only the transitions $1p_{3/2}\rightarrow np_j$. Thus in PWA at 0° ($\Delta L=0$), assuming the radial overlaps for $s_{1/2}\rightarrow s_{1/2}$, $p_{1/2}\rightarrow p_{1/2}$, and $p_{3/2}\rightarrow p_{3/2}$ are about the same, the summed cross section to 0^- states should be roughly two times as large as the $p_{3/2}\rightarrow p_{3/2}$ result. Note, however, that the $s_{1/2}\rightarrow s_{1/2}$ transition will be even more strongly reduced by absorption than the p→p transitions. Thirdly, in Ref. 28, it is assumed that two-body $\bar{p}p$ elastic scattering is isotropic, so a value

$$d\sigma/d\Omega_L(180^\circ)\approx\sigma_{el}/4\pi\approx 6.4 \text{ mb/sr}$$

is assumed. This is an overestimate (by a factor of 2 at $E_{\bar{p}}=150$ MeV, and more at other energies), since the observed $\bar{p}p$ angular distribution is in fact strongly forward peaked. For these reasons we believe that the $^{16}O(\bar{p},p)^{16}_{\bar{p}}C$ cross sections have been qualitatively overestimated in Ref. 28, and we disagree with their conclusion that protons produced by the $(\bar{p},p)$ process should be "clearly distinguishable" from the background for $E_p>100$ MeV.

The crucial question now is whether the protons from the $(\bar{p},p)$ reaction on nuclei are observable at all on top of a large physical background arising from $\bar{p}$ annihilation, followed by secondary proton emission due to pion absorption. This background proton spectrum has been estimated theoretically in the framework of the internuclear cascade model.[29–31] Recently, the $(\bar{p},p)$ reaction has been studied by Garreta *et al.*[4] at LEAR, using ^{12}C, ^{63}Cu, and ^{209}Bi targets. In a companion experiment by DiGiacomo *et al.*,[5] a ^{28}Si target was used. The spectra[4,5] show no clear evidence of a peak which could be identified as an $\bar{N}$-nuclear state. In Ref. 4, a Maxwellian form

$$\left[\frac{d^2\sigma}{d\sigma dE_p}\right]_{bg}=C\sqrt{E_p}e^{-E_p/T} \tag{4.9}$$

was used to parametrize the data. In Eq. (4.9), we use the subscript "bg" to stand for "background." For a ^{12}C target at 0°, they[4] found values $C\approx 80$ μb/sr MeV$^{3/2}$ and $T\approx 86$ MeV. The slope parameter T is somewhat larger than the values $T\approx 60$—65 MeV predicted by the cascade calculations.[29,30] The essentially isotropic angular dependence observed for the emitted protons is consistent with the cascade calculation, however.

We now consider the "signal to background" ratio R defined by

$$R \equiv (d^2\sigma/d\Omega\, dE_p)_{\text{peak}}/(d^2\sigma/d\Omega\, dE_p)_{\text{bg}} . \quad (4.10)$$

The peak cross section $(d^2\sigma/d\Omega\, dE_p)_{\text{peak}}$ for the formation of any particular $\bar{N}$-nuclear bound state specified by the shell model orbit $\{nlj\}$ is obtained from Eq. (4.8) as

$$(d^2\sigma/d\Omega\, dE_p)_{\text{peak}} = \frac{2}{\pi\Gamma}\frac{d\sigma}{d\Omega}(Q_0) . \quad (4.11)$$

Note that the Q dependence of $d\sigma/d\Omega(Q)$ produces only a small shift in the peak position away from $Q=Q_0$, even for broad states, as shown in Fig. 5.

Now consider the transitions $1p_{3/2} \to np_j$ for the $^{16}\text{O}(\bar{p},p)^{16}_{\bar{p}}\text{C}$ reaction. From Eq. (4.11), we find at 0° the values

$$(d^2\sigma/d\Omega\, dE_p)_{\text{peak}} \approx \begin{cases} 3.0 \text{ for } 1p_{3/2} \to 1p_j \\ 2.2 \text{ for } 1p_{3/2} \to 2p_j \\ 9.1 \text{ for } 1p_{3/2} \to 3p_j \end{cases} \quad (4.12)$$

in μb/sr MeV, using the widths Γ from Table II. We now estimate the background from Eq. (4.9), using $T=86$ MeV and $C=95.9$ μb/sr MeV$^{3/2}$. The latter value is obtained by extrapolating to ^{16}O the value $C=80$ μb/sr MeV$^{3/2}$ for ^{12}C, using the observed[4] $A^{0.63}$ dependence of the proton spectrum. We obtain

$$R = \begin{cases} 2.7\times10^{-2}\ (1p_j) \\ 1.1\times10^{-2}\ (2p_j) , \\ 3.8\times10^{-2}\ (3p_j) \end{cases} \quad (4.13)$$

where the background has been evaluated at the energy $E_p = E_{\bar{p}} + Q_0$. Our calculations use $E_{\bar{p}}=150$ MeV; we assume that the background measured[4] at 180 MeV remains essentially the same at 150 MeV.

The "signal to noise" ratios R of Eq. (4.13) would be very difficult if not impossible to detect experimentally. One might hope for a more favorable situation, in which the $\bar{p}$-nucleus real potential is extremely deep in the interior region, while healing to the shallow phenomenological values required in the nuclear surface by $\bar{p}$-atom and $\bar{p}$ elastic scattering data.[1-3,15] This would give rise to high energy protons corresponding to deeply bound $\bar{N}$-nuclear states. However, these protons are necessarily spread over a large energy region of order $\Gamma \approx 2W_0$ and peak cross sections are not expected to exceed the typical values in Eq. (4.12). Using Eq. (4.9), we find that $(d^2\sigma/d\Omega\, dE_p)_{\text{bg}}$ remains above 1 μb/sr MeV for $E_p < 650$ MeV ($\bar{p}$ binding energy of order 500 MeV), so it is unlikely that values $R \sim 1$ are attained, even in extreme cases.

A possible exception to this rather pessimistic viewpoint may be provided by certain $\bar{p}$-atomic states.[8] Our example of the $3p$ quasiatomic state in Eq. (4.13) is typical but unfavorable, in that R is about the same as for the strongly bound states. In certain special cases, an atomic state may have a considerably enhanced formation cross section from the $(\bar{p},p)$ reaction due to a happy coincidence of a sizable radial overlap and a large spectroscopic factor. Such an example has been found by Gibbs and Kaufmann,[8] namely the $^{31}\text{P}(\bar{p},p)^{31}_{\bar{p}}\text{Al}$ reaction. The single particle transition is from the $2s$ proton state (7.3 MeV binding) to the lowest s-wave quasiatomic state, bound by 1.15 MeV with a width $\Gamma=106$ keV. In Ref. 8, a cross section $d\sigma/d\Omega \approx 20$ μb/sr at $E_{\bar{p}}=150$ MeV is given for this state. We have reduced this estimate by a factor 0.52, since the two-body $p\bar{p}$ cross section which was assumed (Table 3 of Ref. 8) disagrees with the original $p\bar{p}$ data at 180° (Table I of Ref. 27). We then obtain at 0°,

$$\begin{aligned} &(d^2\sigma/d\Omega dE_p)_{\text{peak}} \approx 62\ \mu\text{b/sr MeV} , \\ &R \approx 0.2\text{–}0.3 , \end{aligned} \quad (4.14)$$

where the range of R values reflects the uncertainty in the choice of T. Comparing Eq. (4.14) with Eq. (4.13), we see that the R value for the $^{31}_{\bar{p}}\text{Al}$ s-wave atomic state is enhanced by an order of magnitude relative to Eq. (4.13), bringing it into the realm of possible detection at LEAR. Note, however, that we have assumed perfect energy resolution in obtaining Eq. (4.14). The actual resolution $\Delta E \approx 1$ MeV in Ref. 4 is about ten times as large as the natural line width of the quasiatomic state, so we would have to reduce R by a factor of 10. Thus high resolution ($\Delta E \sim 100$ keV) is absolutely essential in searching for the few enhanced quasiatomic $\bar{p}$ states which may exist.

V. ANTINUCLEON BOUND STATES IN LIGHT SYSTEMS

The results presented in Secs. III and IV refer to a $\bar{p}$ bound to a spin-isospin saturated nuclear core ($S_c=0$, $I_c=0$). In this case, the optical potential $\langle V_{\text{opt}}(r)\rangle$ seen by the $\bar{p}$ is proportional to the spin-isospin *averaged* two-body $\bar{p}N$ t-matrix t_0. For a *heavy* nuclear core with spin $S_c \neq 0$ and/or isospin $I_c \neq 0$, the corrections to this averaged $\langle V_{\text{opt}}(r)\rangle$ will generally be rather small [for instance, proportional to $(N-Z)/A$ for the isospin dependent Lane potential]. In the case of a *light* core ($A=2$ or 3 will be considered here), in contrast, the corrections to $\langle V_{\text{opt}}(r)\rangle$ could be rather substantial, particularly since the underlying two-body $N\bar{N}$ interaction is expected to exhibit a sizable spin and isospin dependence. If the $N\bar{N}$ t matrix (complex) is decomposed in the form

$$t(r) = t_0 + t_1 \boldsymbol{\sigma}_{\bar{N}}\cdot\boldsymbol{\sigma}_N + t_2 \boldsymbol{\tau}_{\bar{N}}\cdot\boldsymbol{\tau}_N + t_3 \boldsymbol{\sigma}_{\bar{N}}\cdot\boldsymbol{\sigma}_N \boldsymbol{\tau}_{\bar{N}}\cdot\boldsymbol{\tau}_N \quad (5.1)$$

we obtain a first-order folded optical potential

$$V_{\text{opt}}(r) = \left[At_0 + t_1 \boldsymbol{\sigma}_{\bar{N}}\cdot\langle\boldsymbol{\sigma}_c\rangle + t_2 \boldsymbol{\tau}_{\bar{N}}\cdot\langle\boldsymbol{\tau}_c\rangle + t_3 \left\langle \sum_{i=1}^{A} \boldsymbol{\sigma}_{\bar{N}}\cdot\boldsymbol{\sigma}_i \boldsymbol{\tau}_{\bar{N}}\cdot\boldsymbol{\tau}_i \right\rangle \right] f(r) , \quad (5.2)$$

where $\boldsymbol{\sigma}_c = 2\mathbf{S}_c$, $\boldsymbol{\tau}_c = 2\mathbf{I}_c$, and $f(r)$ is a function obtained by convoluting the nuclear density with the radial dependence of the two-body interaction. For our qualitative discussion, we assume that each component t_i has the same range, and hence $f(r)$ is a common factor in Eq. (5.2).

For a spin-isospin unsaturated core, one may look for two effects, which in some cases may act in unison, i.e., (a) an *attractive* contribution of *one-pion exchange* to $V_{\text{opt}}(r)$, and (b) a *decrease* of the absorptive part, $(\text{Im}\, V_{\text{opt}}/\text{Im}\langle V_{\text{opt}}\rangle) < 1$, due to the altered spin-isospin en-

vironment of the $\bar{N}$. The effect of (a) is to provide a longer range tail to $\mathrm{Re}\,V_{\mathrm{opt}}(r)$, which would help to localize the $\bar{N}$ bound state wave function at larger distances, where it would have less radial overlap with the absorptive potential. The effect of (b) would be to decrease the width Γ of an $\bar{N}$ bound state relative to the value Γ_0 characteristic of the average absorptive potential. For our rough estimates, we use the perturbative result

$$\frac{\Gamma}{\Gamma_0}=\frac{\mathrm{Im}\left[At_0+t_1\boldsymbol{\sigma}_{\bar{N}}\cdot\langle\boldsymbol{\sigma}_c\rangle+t_2\boldsymbol{\tau}_{\bar{N}}\cdot\langle\boldsymbol{\tau}_c\rangle+t_3\left\langle\sum_{i=1}^{A}\boldsymbol{\sigma}_{\bar{N}}\cdot\boldsymbol{\sigma}_i\boldsymbol{\tau}_{\bar{N}}\cdot\boldsymbol{\tau}_i\right\rangle\right]}{A\ \mathrm{Im}t_0}\ . \tag{5.3}$$

The quenching phenomenon for Γ/Γ_0, due to the spin-isospin dependence of absorptive processes, has previously been studied[32] for Σ^- hypernuclei. There, the $\Sigma N\to\Lambda N$ conversion reaction is dominated by the $^3S_1$, $I=\frac{1}{2}$ channel at low energy, so the Σ^--hypernuclear width is suppressed if ΣN pairs in the nucleus are arranged to be predominantly in the $^1S_0$ state. The ${}^6_{\Sigma}$H system provides an example[10] of such a width reduction due to *spin-isospin selectivity.*

We now investigate the possibility of obtaining small values of Γ/Γ_0 for an $\bar{N}$-nuclear system. *A priori*, the situation is much less favorable than for light Σ^- hypernuclei, for two principal reasons: (a) for $\bar{N}$-nuclei, the scale of widths ($\Gamma_0\approx 50$–100 MeV, as per Sec. III) is considerably larger than that for Σ^- hypernuclei ($\Gamma_0\approx 10$–20 MeV for bound states, as per Ref. 32), requiring a more dramatic reduction factor Γ/Γ_0 in order for a state to be observable, and (b) the $\Sigma N\to\Lambda N$ conversion reaction at low energy proceeds almost entirely through *one spin-isospin channel,* a situation which leads to the *maximum* possible reduction ($\Gamma/\Gamma_0\approx 0$) for some spin-isospin configurations [and width enhancement, $(\Gamma/\Gamma_0)>1$, for others]. In contrast, the absorptive $N\bar{N}$ interaction, although it exhibits a sizable spin and isospin dependence in particular models,[9,33–36] is not expected to be overwhelmingly dominated by a *single* spin-isospin channel. In realistic cases, we thus do not anticipate approaching the theoretical limit $\Gamma/\Gamma_0=0$. Conversely, the startling observation of a very narrow $\bar{N}$-nuclear state (non-Coulomb) would constitute strong evidence for an $N\bar{N}$ absorptive interaction dominated by a particular spin and isospin channel.

The available *light targets* for which one might expect to see some effects of spin-isospin nonsaturation are ^{3}H, ^{3}He, and ^{4}He. We consider the reactions

$$A(\bar{p},N)X \tag{5.4}$$

leading to states X of the type

$$X=[\bar{N}+(A-1)N]_{I_x,S_x} \tag{5.5}$$

labeled by the total isospin I_x and spin S_x. We consider systems with all particles in s states, for which the total angular momentum J_x is equal to S_x.

In order to estimate Γ/Γ_0, we assume that the spin-isospin dependence of Imt follows that of the absorptive part of the $N\bar{N}$ *potential* $W(r)$, the central part of which can be parametrized in the form

$$W(r)=(\alpha+\beta\boldsymbol{\sigma}_{\bar{N}}\cdot\boldsymbol{\sigma}_N+\gamma\boldsymbol{\tau}_{\bar{N}}\cdot\boldsymbol{\tau}_N+\delta\boldsymbol{\sigma}_{\bar{N}}\cdot\boldsymbol{\sigma}_N\boldsymbol{\tau}_{\bar{N}}\cdot\boldsymbol{\tau}_N)g(r)\ . \tag{5.6}$$

In Ref. 37, $g(r)$ was taken to be a Woods-Saxon form, and spin-isospin dependence neglected ($\beta=\gamma=\delta=0$). This was sufficient to obtain a good fit to $N\bar{N}$ total elastic, charge exchange, and reaction cross sections. However, a fit to polarization and backward elastic scattering data seem to require the introduction of a spin-isospin dependence for $W(r)$. For instance, the Paris group[9] finds the following ratios of the strengths W_{SI} in different spin-isospin channels at kinetic energy $E\approx 0$, appropriate for a discussion of $\bar{N}$-nuclear bound states:

$$W_{00}:W_{01}:W_{10}:W_{11}=1:0.81:0.11:0.07\ . \tag{5.7}$$

Note that $\{\alpha,\beta,\gamma,\delta\}$ are taken to be energy dependent in Ref. 9, and spin-orbit and tensor contributions are also included. Although the W's grow linearly with E (except for W_{11}, which is assumed constant), the ratios (5.7) are more or less independent of E (at $E=200$ MeV, we find 1:1.12:0.17:0.017). The main *qualitative feature of the Paris model,*[9] as shown by Eq. (5.7), is that *W for $S=0$ is an order of magnitude stronger than for $S=1$,* whereas the isospin dependence is much milder. In an alternative fit to the $N\bar{N}$ data in a coupled channel framework, the Nijmegen group[33] does not require such a strong spin dependence. Estimates based on the quark rearrangement model for $N\bar{N}$ annihilation[34,35] also give stronger absorption for $S=0$ than for $S=1$, but not as dramatic a difference as Eq. (5.7).

If we evaluate Γ/Γ_0 for the two-body $N\bar{N}$ system using Eq. (5.7), the width Γ of the I of the $I=S=1$ states should be considerably suppressed with respect to the "average" width Γ_0, i.e.,

$$\frac{\Gamma}{\Gamma_0}=\frac{W_{11}}{(W_{00}+3W_{01}+3W_{10}+9W_{11})/16}$$
$$=(\alpha+\beta+\gamma+\delta)/\alpha=0.26\ , \tag{5.8}$$

where we have used the numerical values at $E=0$,

$$\frac{\beta}{\alpha}=-0.704,\frac{\gamma}{\alpha}=-0.067,\frac{\delta}{\alpha}=+0.034 \tag{5.9}$$

from the Paris model.[9]

In addition to a suppressed width, the $S=1$, $I=1$ $N\bar{N}$ configuration also benefits from *long range attraction* from one-pion exchange (OPE), which contributes an $N\bar{N}$ potential

$$V_{\mathrm{OPE}}(r)=-\frac{g^2_{\pi NN}}{4\pi}\frac{\mu^3_\pi}{12m^2_N}\boldsymbol{\sigma}_{\bar{N}}\boldsymbol{\sigma}_N\boldsymbol{\tau}_{\bar{N}}\cdot\boldsymbol{\tau}_N\phi(x)\ , \tag{5.10}$$

with $g^2_{\pi NN}/4\pi = 14.4$. Here, μ_π and m_N are the pion and nucleon masses, respectively, and $\phi(x) = e^{-x}/x$ with $x = \mu_\pi r$. In Ref. 38, the Paris model was used to find $N\bar{N}$ resonances by solving the Schrödinger equation. As might be anticipated on the basis of the general arguments given here, relatively narrow ($\Gamma \approx 10$–20 MeV) $I = S = 1$ states (with $L = 1$) were predicted near the $N\bar{N}$ threshold. There is as yet little experimental data on this energy region, which hopefully will be explored at LEAR. Some time ago, evidence for a narrow *bound* state of the $N\bar{N}$ system was found[39] in an experimental study of the $(\bar{p},p)$ reaction on a deuteron target.

After a brief digression on the two-body $N\bar{N}$ problem, we return to the study of three- and four-body $\bar{N}$ states.

A. Three-body $\bar{N}NN$ bound states

We now consider the $(\bar{N},N)$ reactions on the $A = 3$ targets ^3H and ^3He. For a $\bar{p}$ beam, the various channels are

$$^3\mathrm{He}(\bar{p},p)X\ , \tag{5.11a}$$

$$^3\mathrm{H}(\bar{p},p)X\ , \tag{5.11b}$$

$$^3\mathrm{He}(\bar{p},n)X\ , \tag{5.11c}$$

$$^3H(\bar{p},n)X\ . \tag{5.11d}$$

The $\bar{N}NN$ states X have isospin $I_x = \frac{1}{2}$ or $\frac{3}{2}$. For reactions (5.11) with orbital angular momentum transfer $\Delta L = 0$, only states with $J_x = S_x$ will be populated, assuming $L = 0$ for the target. For $\Delta L \neq 0$ transitions, which peak at nonzero angle for the outgoing nucleon, one could also produce $\bar{N}NN$ configurations with relative orbital angular momentum $L \neq 0$ between the $\bar{N}$ and the NN cluster. If such states are bound, they would be longer lived than $L = 0$ states of the same S_x and I_x. Thus *angular distributions* for reactions (5.11) should be measured to look for such $L \neq 0$ states. Our considerations on quenching factors Γ/Γ_0 are independent of L, however.

The NN core for the states X can only have the Pauli-allowed spin-isospin combinations $S_c = 0$, $I_c = 1$ or $S_c = 1$, $I_c = 0$, i.e., the core is either spin or isospin saturated. Consequently,

$$\left\langle \sum_{i=1}^{2} \sigma_{\bar{N}} \cdot \sigma_i \tau_{\bar{N}} \cdot \tau_i \right\rangle = 0 \tag{5.12}$$

and the OPE contribution (5.10) to the real potential between the $\bar{N}$ and the core vanishes. The width ratios Γ/Γ_0 for the $\bar{N}NN$ states are found to be

$$\frac{\Gamma}{\Gamma_0} = \begin{cases} (\alpha - 2\beta)/\alpha \text{ for } S_x = \frac{1}{2}, I_x = \frac{1}{2}, S_c = 1, I_c = 0 \\ (\alpha + \beta)/\alpha \text{ for } S_x = \frac{3}{2}, I_x = \frac{1}{2}, S_c = 1, I_c = 0 \\ (\alpha - 2\gamma)/\alpha \text{ for } S_x = \frac{1}{2}, I_x = \frac{1}{2}, S_c = 0, I_c = 1 \\ (\alpha + \gamma)/\alpha \text{ for } S_x = \frac{1}{2}, I_x = \frac{3}{2}, S_c = 0, I_c = 1\ . \end{cases} \tag{5.13}$$

The values of Γ/Γ_0 are collected in Table VI for the four limiting situations where $W(r)$ is dominated by a single two-body spin-isospin channel $\{S,I\}$, as well as for the more realistic values of Eq. (5.9). One notes immediately that a value $\Gamma/\Gamma_0 = 0$ can only be achieved if $S = 0$ or $I = 0$ channels dominate $W(r)$. This is analogous to results already known for Σ hypernuclei.[32] The Paris model[9] is not too far from a limit in which $S = 0$ two-body annihilation dominates, and there is no isospin dependence of $W(r)$. In this limit, we have

$$\frac{\Gamma}{\Gamma_0} = \begin{cases} 3 \text{ for } \{\frac{1}{2}, \frac{1}{2}, 1, 0\} \\ 0 \text{ for } \{\frac{3}{2}, \frac{1}{2}, 1, 0\} \\ 1 \text{ for } \{\frac{1}{2}, \frac{1}{2}, 0, 1\} \\ 1 \text{ for } \{\frac{1}{2}, \frac{3}{2}, 0, 1\}\ . \end{cases} \tag{5.14}$$

We see from Eq. (5.14) and Table VI, that *the only candidate for a narrow $\bar{N}NN$ state is the one with $S_x = \frac{3}{2}$, $I_x = \frac{1}{2}$, if the $N\bar{N}$ annihilation potential is dominated by the $S = 0$ channel.* This result is easy to understand, if one notes that an $S_x = \frac{3}{2}$ state can only be formed by coupling an $S = 1$ $N\bar{N}$ pair to the extra nucleon, and we have assumed that the annihilation potential operates primarily for $S = 0$. Another interesting limit (far from the Paris model) occurs when $I = 0$ annihilation dominates (independent of the spin mixture), in which case the width of the $S_x = \frac{1}{2}$, $I_x = \frac{3}{2}$ $\bar{N}NN$ state will be strongly quenched (here the $N\bar{N}$ pair must have $I = 1$).

The formalism for calculating the cross sections for the reactions (5.11a)–(5.11d) is given in the Appendix. The laboratory differential cross sections $d\sigma/d\Omega_L$ are of the form

$$\frac{d\sigma}{d\Omega_L} = |N^{(0)}_{1s}(q)|^2 |f|^2\ , \tag{5.15}$$

where $N^{(0)}_{1s}(q)$ is the s-shell form factor for a $\Delta L = 0$ transition, defined in Eq. (A.19), and $|f|^2$ is a factor given by

TABLE VI. Width ratios Γ/Γ_0 for states of the $\bar{N}NN$ system. [The columns labeled with $\{S,I\}$ values refer to the two-body $N\bar{N}$ absorptive channel which is assumed to dominate. The column labeled "Paris" uses the parameters of Eq. (5.9)].

$\bar{N}NN$ state $\{S_x, I_x, S_c, I_c\}$	$S=0, I=0$	$S=0, I=1$	$S=1, I=0$	$S=1, I=1$	Paris
$\frac{1}{2}, \frac{1}{2}, 1, 0$	3	3	$\frac{1}{3}$	$\frac{1}{3}$	2.41
$\frac{3}{2}, \frac{1}{2}, 1, 0$	0	0	$\frac{4}{3}$	$\frac{4}{3}$	0.30
$\frac{1}{2}, \frac{1}{2}, 0, 1$	3	$\frac{1}{3}$	3	$\frac{1}{3}$	1.13
$\frac{1}{2}, \frac{3}{2}, 0, 1$	0	$\frac{4}{3}$	0	$\frac{4}{3}$	0.93

the sums of absolute squares of two-body $N\bar{N}$ amplitudes f_i tabulated in Table VIII in the Appendix. For instance, if we focus attention on the potentially narrow $S_x=\frac{3}{2}$, $I_x=\frac{1}{2}$ state of the $\bar{N}NN$ system, we have

$$|f|^2=\begin{cases}16|b_{\sigma\tau}|^2+32|b_\tau^{TQ}|^2 \text{ for } {}^3\text{He}(\bar{p},p)\\ 4|b_\sigma-b_{\sigma\tau}|^2+8|b_0^{TQ}-b_\tau^{TQ}|^2 \text{ for } {}^3\text{He}(\bar{p},n)\\ 4|b_\sigma+b_{\sigma\tau}|^2+8|b_0^{TQ}+b_\tau^{TQ}|^2 \text{ for } {}^3\text{H}(\bar{p},n)\end{cases} \tag{5.16}$$

for the production of this state in the various reaction channels (5.11). The amplitudes b_i are defined in Eqs. (A8)–(A13) of the Appendix. Note that the ^{3}H($\bar{p}$,p) process does *not* excite the $S_x=\frac{3}{2}$, $I_x=\frac{1}{2}$ state.

The form factor $|N_{1s}^{(0)}(q)|^2$ can be roughly estimated in the eikonal approximation, using an harmonic oscillator wave function for the $A=3$ target with radius parameter $b=1.7$ fm and neglecting the real parts of the $\bar{N}$ and N optical potentials. We find

$$N_{1s}^{(0)}(q=0)\approx\frac{1}{S_{\bar{p}}-S_p}\int_0^\infty dt(e^{-S_p e^{-t}}-e^{-S_{\bar{p}}e^{-t}}), \tag{5.17}$$

where $S_p=3\sigma_p/2\pi b^2\approx 1.09$ and $S_{\bar{p}}=3\sigma_{\bar{p}}/2\pi b^2\approx 2.48$, using $\sigma_{\bar{p}}=150$ mb and $\sigma_p=66$ mb. We then obtain $|N_{1s}^{(0)}(q=0)|^2\approx 0.22$, i.e., a suppression of ($\bar{p}$,N) cross sections due to absorption of about a factor of 4. For convenience in plotting cross sections, we have assumed that $|N_{1s}^{(0)}|^2(p_L/p_{\text{c.m.}})^2\approx 1$. At energies below 100 MeV, the absorption factor is expected to be larger than we have assumed here, thereby suppressing the cross sections somewhat. Note that we have also assumed the existence of an $L=0$ $\bar{N}NN$ bound state with an $\bar{N}$ binding energy comparable to that of a nucleon bound in the target, so that the radial overlap of the N and $\bar{N}$ wave functions will be of order unity.

The energy dependence of the 0° laboratory differential cross sections for the production of the $S_x=\frac{3}{2}$, $I_x=\frac{1}{2}$, $\bar{N}NN$ state in the ($\bar{p}$,N) reactions on an $A=3$ target are shown in Fig. 6. The difference between curves B and B' indicates the effect of tensor $N\bar{N}$ amplitudes for the ^{3}He ($\bar{p}$,p)X reaction. For this case [as well as the ($\bar{p}$,p) reaction on other targets], the tensor forces produce only a modest increase in cross section, while for the ($\bar{p}$,n) process, the tensor terms are much more important.

From Fig. 6, we see that the ^{3}H($\bar{p}$,n)X reaction in the vicinity of $E_{\bar{p}}=175$ MeV has the largest cross section (0.8–0.9 mb/sr) for the production of X ($S_x=\frac{3}{2}$, $I_x=\frac{1}{2}$). However, this process would be difficult to study experimentally. The experimental situation for the ^{3}He($\bar{p}$,p)X reaction would be much more favorable. For this case, we estimate a signal to background ratio

$$R\approx 5/\Gamma \text{ (MeV)} \tag{5.18}$$

at $E_{\bar{p}}=150$ MeV. This estimate was obtained by extrapolating the measured background[4] of Eq. (4.9) to an $A=3$ target; this yielded $(d^2\sigma/d\Omega\, dE_p)_{bg}\approx 70$ μb/sr MeV. From Eq. (5.18), we note that R remains larger than 0.2 (presumably a measurable signal) if $\Gamma<25$ MeV. Thus if X ($S_x=\frac{3}{2}$, $I_x=\frac{1}{2}$) is indeed a narrow state, it seems feasible to search for it at LEAR in the ^{3}He($\bar{p}$,p)X reaction at energies $E_{\bar{p}}\approx 100$–200 MeV.

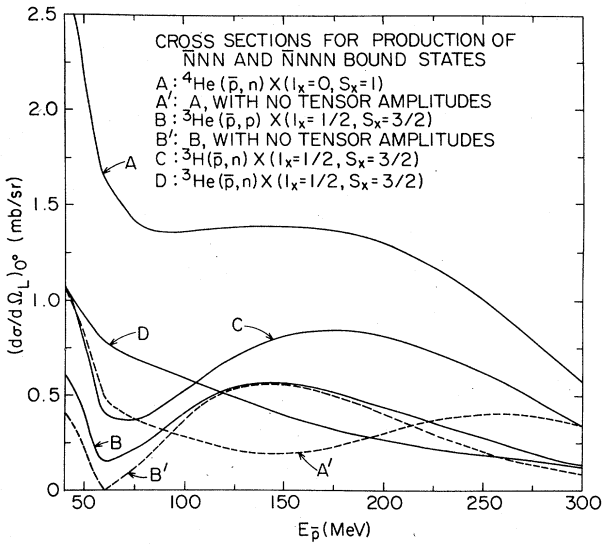

FIG. 6. Forward angle laboratory cross sections as a function of $\bar{p}$ laboratory energy for producing potentially narrow $\bar{N}NN$ ($S_x=\frac{3}{2}$, $I_x=\frac{1}{2}$) and $\bar{N}NNN$ ($S_x=1$, $I_x=0$) bound states in ($\bar{p}$,N) reactions on $A=3$ and 4 targets.

B. Four-body $\bar{N}NNN$ bound states

We now consider the possibility of relatively stable $\bar{N}NNN$ four-body states X and their production in the reactions

$$^4\text{He}(\bar{p},p)X\ , \tag{5.19a}$$

$$^4\text{He}(\bar{p},n)X\ . \tag{5.19b}$$

Unlike the $\bar{N}NN$ states, the four-body states can benefit from an attraction in some channels due to one-pion exchange, since the $A=3$ core is *both* spin and isospin unsaturated. We find

$$\left\langle\sum_{i=1}^{3}\boldsymbol{\sigma}_{\bar{N}}\cdot\boldsymbol{\sigma}_i\boldsymbol{\tau}_{\bar{N}}\cdot\boldsymbol{\tau}_i\right\rangle=-\boldsymbol{\sigma}_{\bar{N}}\cdot\boldsymbol{\sigma}_c\boldsymbol{\tau}_{\bar{N}}\cdot\boldsymbol{\tau}_c \tag{5.20}$$

so that the OPE potential of Eq. (5.10) gives rise to a contribution $\Delta V_{\text{OPE}}(r)$ to the real part of the $\bar{N}$-core optical potential of the form

$$\Delta V_{\text{OPE}}(r)=\frac{g_{\pi NN}^2\mu_\pi^3}{4\pi 12m_N^2}\boldsymbol{\sigma}_{\bar{N}}\cdot\boldsymbol{\sigma}_c\boldsymbol{\tau}_{\bar{N}}\cdot\boldsymbol{\tau}_c J(r)\ , \tag{5.21}$$

where $J(r)$ is the average of the Yukawa function over the three-body core density $\rho(\boldsymbol{\rho},\boldsymbol{\lambda})$:

$$J(r)=\frac{\int d^3\rho\, d^3\lambda\,\rho(\boldsymbol{\rho},\boldsymbol{\lambda})e^{-\mu_\pi|\mathbf{r}+\sqrt{2/3}\boldsymbol{\lambda}|}/\mu_\pi|\mathbf{r}+\sqrt{2/3}\boldsymbol{\lambda}|}{\int d^3\rho\, d^3\lambda\,\rho(\boldsymbol{\rho},\boldsymbol{\lambda})}, \tag{5.22}$$

where $\boldsymbol{\rho}=(\mathbf{r}_1-\mathbf{r}_2)/\sqrt{2}$ and $\boldsymbol{\lambda}=(\mathbf{r}_1+\mathbf{r}_2-2\mathbf{r}_3)/\sqrt{6}$ are the usual *relative* coordinates for the three-body system. To evaluate $\Delta V_{\text{OPE}}(r)$, we adopt a Gaussian approximation for $\rho(\boldsymbol{\rho},\boldsymbol{\lambda})$:

$$\rho(\boldsymbol{\rho},\lambda)=ce^{-(\rho^2+\lambda^2)/b^2}, \tag{5.23}$$

where $b=1.7$ fm is chosen to reproduce the rms radius of ^{3}He. The integral $J(r)$ is then given by

$$J(r)=\frac{e^{y/2}}{2x}\left\{e^{-x}\mathrm{erfc}\left[\frac{1}{\sqrt{2y}}(y-x)\right]-e^{x}\mathrm{erfc}\left[\frac{1}{\sqrt{2y}}(y+x)\right]\right\}, \tag{5.24}$$

where

$$\mathrm{erfc}(z)=2/\sqrt{\pi}\int_z^\infty e^{-t^2}dt$$

and $x=\mu_\pi r$, $y=\mu_\pi^2 b^2/3\approx 0.472$. For large r, $J(r)$ assumes the simpler form

$$J(r)\approx e^{y/2}\frac{e^{-x}}{x} \tag{5.25}$$

displaying the same radial dependence as OPE.

The same folding model can be used to construct an estimate of the absorptive part $\mathrm{Im}\,V_{\mathrm{opt}}(r)$ from the two-body $W(r)$. Using a Yakawa form

$$g(r)=\exp(-2m_{\mathrm{N}}r)/2m_{\mathrm{N}}r$$

in Eq. (5.6), which has the same volume integral as the function

$$g(r)=K_0(2m_{\mathrm{N}}r)/2m_{\mathrm{N}}r$$

adopted by the Paris group,[9] we can use Eq. (5.24), with $y=4m_{\mathrm{N}}^2b^2/3\approx 87.13$ to obtain $\mathrm{Im}\,V_{\mathrm{opt}}(r)$. The expansion

$$J(r)\approx\left[\frac{2y}{\pi}\right]^{1/2}\frac{e^{-x^2/2y}}{y^2-x^2}\left[1-y\frac{(3y^2+x^2)}{(y^2-x^2)^2}+\cdots\right], \tag{5.26}$$

valid for $y\gg x$, is appropriate in this case. We note that now $J(r)$ follows the Gaussian radial dependence of the core density rather than that of the two-body interaction as in Eq. (5.25).

Inspection of Eq. (5.21) discloses that *OPE gives an attractive contribution to the $\overline{N}+NNN$ potential for* $S_x=0$, $I_x=1$ or $S_x=1$, $I_x=0$. The values of $\Delta V_{\mathrm{OPE}}(r)$ are given in Fig. 7 as a function of r, along with the estimate of the radial shape of $\mathrm{Im}\,V_{\mathrm{opt}}(r)$ based on Eq. (5.26). For $r\approx b$, the OPE contributes a non-negligible attraction of a few MeV, which would help to localize the $\overline{\mathrm{N}}$ bound state wave function in the surface region, where the absorptive potential is decreasing more rapidly than the OPE piece. This surface localization would tend to decrease the decay width of the $\overline{\mathrm{N}}+\mathrm{NNN}$ state.

The discussion of the width factors Γ/Γ_0 proceeds as in Sec. V A. The $\overline{\mathrm{N}}\mathrm{NNN}$ states can have $S_x=0$, 1 and $I_x=0,1$. For the four possible combinations, we have

$$\frac{\Gamma}{\Gamma_0}=\begin{cases}(\alpha-\beta-\gamma-3\delta)/\alpha \text{ for } S_x=0,I_x=0\\(\alpha+\beta/3-\gamma+\delta)/\alpha \text{ for } S_x=1,I_x=0\\(\alpha-\beta+\gamma/3+\delta)/\alpha \text{ for } S_x=0,I_x=1\\(\alpha+\beta/3+\gamma/3-\delta/3)/\alpha \text{ for } S_x=1,I_x=1\ .\end{cases} \tag{5.27}$$

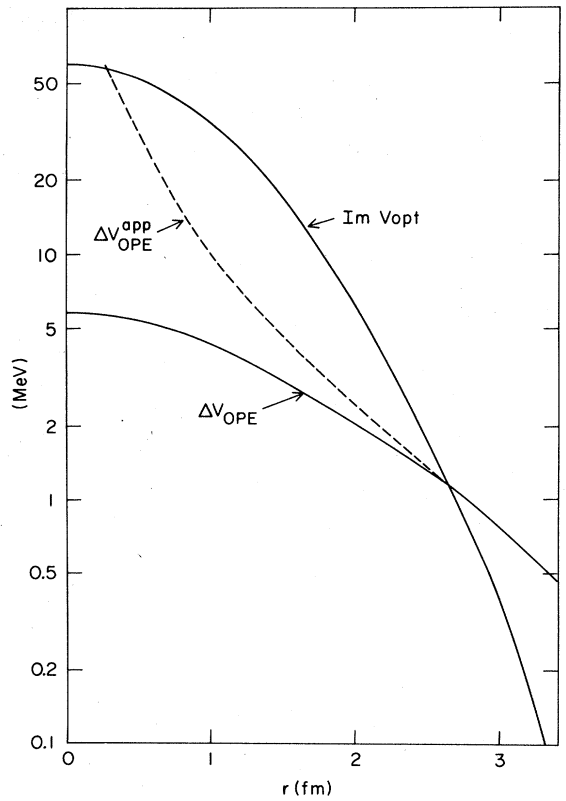

FIG. 7. The absolute magnitude of the contribution ΔV_{OPE} of one-pion exchange to the real part of the $\overline{\mathrm{N}}+\mathrm{NNN}$ optical potential for total spin-isospin $S_x=0$, $I_x=1$ or $S_x=1$, $I_x=0$. The dashed curve for $V_{\mathrm{OPE}}^{\mathrm{app}}$ represents the approximation of Eq. (5.25), and shows how ΔV_{OPE} follows the radial dependence of OPE in the surface region ($r>b$), and the form of the three-nucleon core density for $r<b$. The curve labeled $\mathrm{Im}\,V_{\mathrm{opt}}$ represents the magnitude of the absorptive part of the $\overline{\mathrm{N}}+\mathrm{NNN}$ optical potential scaled to reproduce the well depth $W_0=61$ MeV at $r=0$ found by Garreta *et al.* (Ref. 1) in an analysis of low energy $\bar{\mathrm{p}}$-^{12}C scattering.

The values of Γ/Γ_0 are displayed in Table VII for the four limiting cases where a simple $\{S,I\}$ channel dominates the $\mathrm{N}\overline{\mathrm{N}}$ absorptive potential, as well as the predictions based on Eq. (5.9). Here, unlike the $\overline{\mathrm{N}}\mathrm{NNN}$ case, the dominance of a *single* $\mathrm{N}\overline{\mathrm{N}}$ channel is required to obtain $\Gamma/\Gamma_0=0$. For $S=0$ dominance (no isospin dependence), we obtain

$$\frac{\Gamma}{\Gamma_0}=\begin{cases}\frac{2}{3} \text{ for } S_x=1,I_x=0,1\\2 \text{ for } S_x=0,I_x=0,1\end{cases} \tag{5.28}$$

which is to be compared with Eq. (5.14). The results for the Paris model[9] in Table VII are rather close to the limit (5.28). Thus we do not anticipate major deviations of Γ/Γ_0 from unity for $\overline{\mathrm{N}}\mathrm{NNN}$ systems. Based on the Paris $W(r)$, *the best candidates for relatively narrow $\overline{N}NNN$ states would have $S_x=1$, $I_x=1$ or $I_x=0$,* for which there

TABLE VII. Width ratios Γ/Γ_0 for $\bar{N}NNN$ states. (The columns are labeled as in Table IV.)

$\bar{N}NNN$ State $\{S_x,I_x\}$	$S=0,I=0$	$S=0,I=1$	$S=1,I=0$	$S=1,I=1$	Paris
0,0	0	$\frac{8}{3}$	$\frac{8}{3}$	0	1.67
1,0	$\frac{8}{3}$	0	$\frac{16}{9}$	$\frac{8}{9}$	0.87
0,1	$\frac{8}{3}$	$\frac{16}{9}$	0	$\frac{8}{9}$	1.72
1,1	0	$\frac{8}{9}$	$\frac{8}{9}$	$\frac{32}{27}$	0.73

is a modest reduction in Γ/Γ_0 and where, for the latter case, the OPE contribution to the real potential is attractive. To produce these objects, the reactions (5.19a) and (5.19b) are appropriate. States with $I_x=1$ can be excited in both $(\bar{p},p)$ and $(\bar{p},n)$ reactions, whereas $I_x=0$ states are populated only in the $(\bar{p},n)$ process. From Table IX, we have

$$\frac{d\sigma}{d\Omega_L}=|N_{1s}^{(0)}(q)|^2\begin{cases}(24\,|\,b_{\sigma\tau}\,|^2+48\,|\,b_\tau^{TQ}\,|^2)\text{ for }{}^4\text{He}(\bar{p},p)X\ (I_x=1,S_x=1) & (5.29a)\\ (12\,|\,b_\sigma\,|^2+24\,|\,b_0^{TQ}\,|^2)\text{ for }{}^4\text{He}(\bar{p},n)X\ (I_x=0,S_x=1) & (5.29b)\end{cases}$$

where the form factor N and the amplitudes b_i are defined in the Appendix. We note that the $(\bar{p},p)$ cross section of Eq. (5.29a) is $\frac{3}{2}$ times the $^3\text{He}(\bar{p},p)$ cross section (curve B) in Fig. 6. The $(\bar{p},n)$ cross section (5.29b) is shown in fig. 6 as curve A. In this case, the influence of the tensor amplitude b_0^{TQ} is enormous (compare curves A and A'). At 0° we thus obtain

$$R\approx 10/\Gamma\ (\text{MeV})\ , \tag{5.30}$$

for $^4\text{He}(\bar{p},n)$ at $E_{\bar{p}}=150$ MeV, using the same approximations applied to obtain Eq. (5.18). The estimate (5.30) refers to an s-wave $\bar{N}NNN$ bound state, for which the cross section peaks at 0° ($\Delta L=0$). One should keep in mind the possibility of longer-lived $L\neq 0$ states which would be optimally produced at nonzero angles. In summary, the reactions $^3\text{He}(\bar{p},p)$ and $^4\text{He}(\bar{p},N)$ appear to be good candidates for experimental study at LEAR. They may provide a *test of the strong spin dependence ($S=0$ dominance) of the $N\bar{N}$ annihilation potential* predicted by the Paris group, assuming that the widths Γ in some cases are small enough ($\Gamma<25$ MeV) so that the $\bar{N}$-nuclear states can be observed. Note that other models, for instance due to the Nijmegen[33] and Helsinki[35] groups, predict a different pattern of spin-isospin dependence for $W(r)$. For these models, the spin dependence of $W(r)$ is more modest, and a less dramatic quenching factor Γ/Γ_0 is expected for the $S_x=\frac{3}{2}$, $I_x=\frac{1}{2}$, $\bar{N}NN$ state, for instance. It is worth mentioning that Shapiro and his collaborators[42] have also presented estimates of the binding energies and widths of $\bar{N}NN$ states, for a spin-isospin independent $W(r)$. Here, we have rather emphasized the role of possible *spin-isospin selectivity* in $W(r)$ in reducing the widths of certain configurations.

VI. SUMMARY

We have discussed the energy spectrum of nuclei containing a single antinucleon and estimated their formation cross sections via the $(\bar{N},N)$ reactions on nuclear targets. Except for the quasiatomic $\bar{p}$ states, the bound $\bar{N}$-nuclear excitations are quite unstable in general, with annihilation widths of order $\Gamma\approx 50$—100 MeV. Their binding energies are very sensitive to the depth of the $\bar{N}$-nucleus optical potential in the nuclear interior, which is poorly determined by $\bar{p}$-atom and low energy $\bar{p}$-scattering data. The shallow real potentials favored by recent phenomenological studies[1,2,15] support only a few bound $\bar{N}$ states (non-Coulomb). The cross sections $d^2\sigma/d\Omega\,dE_p$ for the formation of these states in ^{16}O assume peak values of order 1—10 μb/sr MeV, which is much smaller than the annihilation background[4,5] of 100—200 μb/sr MeV. These broad $\bar{N}$-nuclear excitations will thus be very difficult to detect experimentally. For particular $\bar{p}$-atomic states,[8] on the other hand, the "signal/background" ratio of cross sections $d^2\sigma/d\Omega dE_p$ could be as large as 0.2—0.3, although it is more typically of order 1—5×10^{-2}, as for strongly bound $\bar{N}$ states. Excellent energy resolution ($\Gamma\sim 100$ keV) would be required for the detection of quasiatomic $\bar{p}$ states.

We have also considered the possibility that particular configurations of an $\bar{N}$ plus a light spin-isospin unsaturated nuclear core could be anomalously narrow, due to a strong spin-isospin dependence of the $N\bar{N}$ absorptive potential W, or the influence of a nonzero contribution of one-pion exchange to the $\bar{N}$-core Hartree potential. For the Paris model,[9] in which the spin-singlet W dominates, we predict that the $\bar{N}NN$ configuration with spin $S_x=\frac{3}{2}$ and isospin $I_x=\frac{1}{2}$ is the best candidate to be narrow. Configurations of the $\bar{N}NNN$ system with $\{S_x,I_x\}=\{1,0\}$ or $\{1,1\}$ enjoy a more modest width suppression factor Γ/Γ_0, the former having an attractive contribution of one-pion exchange to the $\bar{N}$ Hartree field. The most promising reaction for study appears to be $^3\text{He}(\bar{p},p)X$ in the kinetic energy range $E_{\bar{p}}\simeq 100$—200 MeV. The signal/background ratio for the $S_x=\frac{3}{2}$, $I_x=\frac{1}{2}$ $\bar{N}NN$ states is estimated to be about $5/\Gamma$ (MeV), so narrow excitations with $\Gamma<25$ MeV or so have a reasonable chance of being detected in the presence of the background of nu-

cleon emission induced by $\bar{N}$ annihilation in the target. Even in the absence of a width suppression effect, the light targets ^{3}He and ^{4}He, particularly the former, are the most favorable cases for $\bar{N}$ bound state searches, since the background (which varies essentially as $A^{2/3}$) is minimized relative to the signal.

This work was supported in part by the U. S. Department of Energy under Contract No. DE-AC02-76CH00016 and in part by the U. S.-Israel Binational Science Foundation.

APPENDIX: EXPRESSIONS FOR $(\bar{p},p)$ AND $(\bar{p},n)$ CROSS SECTIONS ON NUCLEAR TARGETS

The input to the $(\bar{p},N)$ nuclear amplitudes considered in the main text consists of the *forward* (0°) $\bar{N}N\to N\bar{N}$ amplitude in the two-body *laboratory* (lab) system

$$f(\bar{N}N\to N\bar{N})_{0^\circ}=b_0+b_\tau\tau_1\cdot\tau_2+b_\sigma\sigma_1\cdot\sigma_2+b_{\sigma\tau}\sigma_1\cdot\sigma_2\tau_1\cdot\tau_2+(b_0^{TQ}+b_\tau^{TQ}\tau_1\cdot\tau_2)S_{12}(\hat{Q}) , \tag{A1}$$

where

$$S_{12}(\hat{Q})=3\sigma_1\cdot\hat{\mathbf{Q}}\sigma_2\cdot\hat{\mathbf{Q}}-\sigma_1\cdot\sigma_2 ,$$
$$\mathbf{Q}=(\mathbf{p}_i^{\bar{N}}+\mathbf{p}_f^{N})/\hbar . \tag{A2}$$

Note that at 0° we have $\mathbf{p}_f^{N}=\mathbf{p}_i^{\bar{N}}$, and we denote this common vector by $\mathbf{p}_L$. Thus, for the two-body cross sections of interest we have

$$\frac{d\sigma}{d\Omega_L}(\bar{p}p\to p\bar{p})_{0^\circ}=4(|b_\tau|^2+3|b_{\sigma\tau}|^2+6|b_\tau^{TQ}|^2) , \tag{A3}$$

$$\frac{d\sigma}{d\Omega_L}(\bar{p}p\to n\bar{n})_{0^\circ}=(|b_0-b_\tau|^2+3|b_\sigma-b_{\sigma\tau}|^2+6|b_0^{TQ}-b_\tau^{TQ}|^2) , \tag{A4}$$

$$\frac{d\sigma}{d\Omega_L}(\bar{p}n\to n\bar{p})_{0^\circ}=(|b_0+b_\tau|^2+3|b_\sigma+b_{\sigma\tau}|^2+6|b_0^{TQ}+b_\tau^{TQ}|^2) . \tag{A5}$$

On the other hand, the theoretical and experimental information on nucleon-antinucleon interactions is summarized[41] by extracting the two-body *center of mass* (c.m.) t matrix. In particular, for *backward* (180°) elastic scattering in the c.m. system.

$$t(\bar{N}N\to\bar{N}N)_{180^\circ}=t_0+t_\tau\tau_1\cdot\tau_2+t_\sigma\sigma_1\cdot\sigma_2+t_{\sigma\tau}\sigma_1\cdot\sigma_2\tau_1\cdot\tau_2+(t_0^{Tq}+t_\tau^{Tq}\tau_1\cdot\tau_2)S_{12}(\hat{q}) , \tag{A6}$$

where

$$\mathbf{q}=(\mathbf{p}_i-\mathbf{p}_f)/\hbar . \tag{A7}$$

Note that at 180° we have $\mathbf{p}_f=-\mathbf{p}_i$. We denote $\mathbf{p}_i$ by $\mathbf{p}_{\text{c.m.}}$. Thus $\mathbf{p}_{\text{c.m.}}$, $\mathbf{q}$, $\mathbf{Q}$, and $\mathbf{p}_L$ are all parallel. Clearly, the amplitudes describing $\bar{N}N\to N\bar{N}$ at 0° and $\bar{N}N\to\bar{N}N$ at 180° must be equal to each other up to a phase $(-1)^{S+I}$ which depends on the s-channel spin and isospin. This requirement leads to the following expressions of the b's in terms of t's:

$$b_0=\frac{\gamma}{4}(t_0+3t_\tau+3t_\sigma+9t_{\sigma\tau}) , \tag{A8}$$

$$b_\tau=\frac{\gamma}{4}(t_0-t_\tau+3t_\sigma-3t_{\sigma\tau}) , \tag{A9}$$

$$b_\sigma=\frac{\gamma}{4}(t_0+3t_\tau-t_\sigma-3t_{\sigma\tau}) , \tag{A10}$$

$$b_{\sigma\tau}=\frac{\gamma}{4}(t_0-t_\tau-t_\sigma+t_{\sigma\tau}) , \tag{A11}$$

$$b_0^{TQ}=\frac{\gamma}{2}(t_0^{Tq}+3t_\tau^{Tq}) , \tag{A12}$$

$$b_\tau^{TQ}=\frac{\gamma}{2}(t_0^{Tq}-t_\tau^{Tq}) , \tag{A13}$$

where

$$\gamma=\lambda\left[\frac{p_L}{p_{\text{c.m.}}}\right] ,$$
$$\lambda=-\epsilon/(4\pi\hbar^2c^2) ,$$
$$\epsilon^2=(mc^2)^2+(cp_{\text{c.m.}})^2 . \tag{A14}$$

The factor λ is a kinematical factor transforming t into $f_{\text{c.m.}}$ and the factor $(p_L/p_{\text{c.m.}})$ transforms $f_{\text{c.m}}(0^\circ)$ to $f_L(0^\circ)$. Equations (A8—A13) demonstrate how each of the definite spin and isospin (t-channel) transfer amplitudes, which are given by the coefficients b, is a *mixture* of various spin and isospin $N\bar{N}$ elastic amplitudes. For example, the $\bar{p}p\to p\bar{p}$ forward cross section (A3) (which is given in terms of purely isovector transfer amplitudes) is expressed in terms of isoscalar and isovector s-channel amplitudes:

$$\frac{d\sigma}{d\Omega_L}(\bar{p}p\to p\bar{p})_{0^\circ}=(p_L/p_{\text{c.m.}})^2\frac{d\sigma}{d\Omega_{\text{c.m.}}}(\bar{p}p\to\bar{p}p)_{180^\circ}=\gamma^2(|t_0-t_\tau|^2+3|t_\sigma-t_{\sigma\tau}|^2+6|t_0^{Tq}-t_\tau^{Tq}|^2) . \tag{A15}$$

Similar expression for other projectiles have been given in the appendices of Refs. 40 and 43.

We record here the general $(\bar{p},N)$ amplitudes in light (s-shell) nuclei. The derivation follows closely that in Ref. 43, leading to Eq. (A15) there. Neglecting recoil corrections we obtain the following amplitudes for the $\Delta L=0$ transition from the ground state with spin and isospin (S_i,I_i) of the nuclear A-body target ($A=2,3,4$) to the state (S_x,I_x) built on a core with (S_c,I_c):

TABLE VIII. Reduced cross sections[a] for the ^{3}He($\bar{p}$,N)X_{I_x,S_x} reaction.

$I_x(I_c)$	$S_x(S_c)$	$(d\sigma/d\Omega_L)/\lvert N_{1s}^{(0)}(q)\rvert^2$ ($\bar{p}$,p)	($\bar{p}$,n)
$\frac{1}{2}(0)$	$\frac{1}{2}(1)$	$6\lvert b_\tau\rvert^2+2\lvert b_{\sigma\tau}\rvert^2+4\lvert b_\tau^{TQ}\rvert^2$	$\frac{3}{2}\lvert b_0-b_\tau\rvert^2+\frac{1}{2}\lvert b_\sigma-b_{\sigma\tau}\rvert^2+\lvert b_0^{TQ}-b_\tau^{TQ}\rvert^2$
$\frac{1}{2}(1)$	$\frac{1}{2}(0)$	$\frac{2}{3}\lvert b_\tau\rvert^2+2\lvert b_{\sigma\tau}\rvert^2+4\lvert b_\tau^{TQ}\rvert^2$	$\frac{3}{2}\lvert b_0+\frac{1}{3}b_\tau\rvert^2+\frac{9}{2}\lvert b_\sigma+\frac{1}{3}b_{\sigma\tau}\rvert^2+9\lvert b_0^{TQ}+\frac{1}{3}b_\tau^{TQ}\rvert^2$
$\frac{3}{2}(1)$	$\frac{1}{2}(0)$	$\frac{4}{3}\lvert b_\tau\rvert^2+4\lvert b_{\sigma\tau}\rvert^2+8\lvert b_\tau^{TQ}\rvert^2$	$\frac{4}{3}\lvert b_\tau\rvert^2+4\lvert b_{\sigma\tau}\rvert^2+8\lvert b_\tau^{TQ}\rvert^2$
$\frac{1}{2}(0)$	$\frac{3}{2}(1)$	$16\lvert b_{\sigma\tau}\rvert^2+32\lvert b_\tau^{TQ}\rvert^2$	$4\lvert b_\sigma-b_{\sigma\tau}\rvert^2+8\lvert b_0^{TQ}-b_\tau^{TQ}\rvert^2$

[a]The ^{3}H($\bar{p}$,n) cross sections are obtained from the tabulated ^{3}He($\bar{p}$,n) cross sections by changing *all* the relative phases between isoscalar and isovector coefficients. The ($\bar{p}$,p) reaction on ^{3}H excites only the $I_x=\frac{3}{2}$ state, with a reduced cross section $4\lvert b_\tau\rvert^2+12\lvert b_{\sigma\tau}\rvert^2+24\lvert b_\tau^{TQ}\rvert^2$.

$$\frac{d\sigma}{d\Omega_L}(\bar{p},p)=48A(2I_i+1)(2I_x+1)\begin{bmatrix} I_x & 1 & I_i \\ -i_x & -1 & i_i \end{bmatrix}^2\begin{Bmatrix} \frac{1}{2} & I_x & I_c \\ I_i & \frac{1}{2} & 1 \end{Bmatrix}^2[S_c,I_c\,|\,\}S_i,I_i]^2\frac{(2S_x+1)}{2}$$

$$\times\sum_{k_s=0,1}(2k_s+1)\begin{Bmatrix} \frac{1}{2} & S_x & S_c \\ S_i & \frac{1}{2} & k_s \end{Bmatrix}^2(\lvert b_c^{(1,k_s)}\rvert^2+2\lvert b_{TQ}^{(1,k_s)}\rvert^2)\lvert N_{1s}^{(0)}(q)\rvert^2, \tag{A16}$$

$$\frac{d\sigma}{d\Omega_L}(\bar{p},n)=4A[S_c,I_c\,|\,\}S_i,I_i]^2\frac{(2S_x+1)}{2}$$

$$\times\sum_{k_s=0,1}(2k_s+1)\begin{Bmatrix} \frac{1}{2} & S_x & S_c \\ S_i & \frac{1}{2} & k_s \end{Bmatrix}^2\Bigg|\Bigg|\delta_{I_iI_x}b_c^{(0,k_s)}-\sqrt{6}b_c^{(1,k_s)}(-1)^{I_x-i_x}\begin{bmatrix} I_x & 1 & I_i \\ -i_x & 0 & i_i \end{bmatrix}$$

$$\times(-1)^{I_x+I_c-\frac{1}{2}}(2I_i+1)^{1/2}(2I_x+1)^{1/2}\begin{Bmatrix} \frac{1}{2} & I_x & I_c \\ I_i & \frac{1}{2} & 1 \end{Bmatrix}\Bigg|^2$$

$$+2\Bigg|\delta_{I_iI_x}b_{TQ}^{(0,k_s)}-\sqrt{6}b_{TQ}^{(1,k_s)}(-1)^{I_x-i_x}\begin{bmatrix} I_x & 1 & I_i \\ -i_x & 0 & i_i \end{bmatrix}$$

$$\times(-1)^{I_x+I_c-\frac{1}{2}}(2I_i+1)^{1/2}(2I_x+1)^{1/2}\begin{Bmatrix} \frac{1}{2} & I_x & I_c \\ I_i & \frac{1}{2} & 1 \end{Bmatrix}\Bigg|^2\Bigg|\lvert N_{1s}^{(0)}(q)\rvert^2, \tag{A17}$$

where

$$b_c^{(0,0)}=b_0,\quad b_c^{(0,1)}=b_\sigma,\quad b_c^{(1,0)}=b_\tau,$$
$$b_c^{(1,1)}=b_{\sigma\tau},\quad b_{TQ}^{(0,k_s)}=b_0^{TQ}\delta_{k_s1}, \tag{A18}$$
$$b_{TQ}^{(1,k_s)}=b_\tau^{TQ}\delta_{k_s1},$$

$[\,|\,\}]$ is the appropriate spin-isospin fractional parentage coefficient, and

TABLE IX. Reduced cross sections for the ^{4}He($\bar{p}$N)X_{I_x,S_x} reaction.

I_x	S_x	$(d\sigma/d\Omega_L)/\lvert N_{1s}^{(0)}(q)\rvert^2$ ($\bar{p}$,p)	($\bar{p}$,n)
0	0		$4\lvert b_0\rvert^2$
1	0	$8\lvert b_\tau\rvert^2$	$4\lvert b_\tau\rvert^2$
0	1		$12\lvert b_\sigma\rvert^2+24\lvert b_0^{TQ}\rvert^2$
1	1	$24\lvert b_{\sigma\tau}\rvert^2+48\lvert b_\tau^{TQ}\rvert^2$	$12\lvert b_{\sigma\tau}\rvert^2+24\lvert b_\tau^{TQ}\rvert^2$

TABLE X. Cross sections $d\sigma/d\Omega_L$ for the $^{16}O(\bar{p},p)^{16}_{\bar{p}}C$ reaction.

J^π	$(p_{3/2}^{-1},p_{3/2})$	$(p_{3/2}^{-1},p_{1/2})$
0^-	$16\,\lvert b_\tau\rvert^2\,\lvert N_{1p}^{(0)}\rvert^2$	
1^-	$\frac{80}{3}(\lvert b_{\sigma\tau}\rvert^2+2\,\lvert b_\tau^{TQ}\rvert^2)\,\lvert N_{1p}^{(0)}\rvert^2+\frac{32}{15}[\lvert b_{\sigma\tau}\rvert^2+3\,\lvert b_\tau^{TQ}\rvert^2+2\mathrm{Re}(b_{\sigma\tau}b_\tau^{TQ*})]\lvert N_{1p}^{(2)}\rvert^2$	$\frac{64}{3}(\lvert b_{\sigma\tau}\rvert^2+2\,\lvert b_\tau^{TQ}\rvert^2)\,\lvert N_{1p}^{(0)}\rvert^2+\frac{8}{3}[\lvert b_{\sigma\tau}\rvert^2+3\,\lvert b_\tau^{TQ}\rvert^2+2\mathrm{Re}(b_{\sigma\tau}b_\tau^{TQ*})]$
	$+\frac{64}{3}[\lvert b_\tau^{TQ}\rvert^2+2\mathrm{Re}(b_{\sigma\tau}b_\tau^{TQ*})]\mathrm{Re}(N_{1p}^{(0)}N_{1p}^{(2)*})$	$\times\lvert N_{1p}^{(2)}\rvert^2-\frac{64}{3}[\lvert b_\tau^{TQ}\rvert^2+2\mathrm{Re}(b_{\sigma\tau}b_\tau^{TQ*})]\mathrm{Re}(N_{1p}^{(0)}N_{1p}^{(2)*})$
2^-	$16\,\lvert b_\tau\rvert^2\,\lvert N_{1p}^{(2)}\rvert^2$	$8[2\,\lvert b_\tau\rvert^2+3\,\lvert b_{\sigma\tau}\rvert^2+3\,\lvert b_\tau^{TQ}\rvert^2-6\mathrm{Re}(b_{\sigma\tau}b_\tau^{TQ*})]\,\lvert N_{1p}^{(2)}\rvert^2$
3^-	$\frac{48}{5}[7\,\lvert b_{\sigma\tau}\rvert^2+16\,\lvert b_\tau^{TQ}\rvert^2+4\,\mathrm{Re}(b_{\sigma\tau}b_\tau^{TQ*})]\,\lvert N_{1p}^{(2)}\rvert^2$	

$$N_{1s}^{(0)}(q)=\int d^3r\,\psi_{\bar{p}}^{(-)*}(\mathbf{p}'_L,\mathbf{r})\rho_{fi}(\mathbf{r})\psi_{\bar{p}}^{(+)}(\mathbf{p}_L,\mathbf{r})\,,\qquad \mathbf{q}=\mathbf{p}_L-\mathbf{p}'_L\,, \tag{A19}$$

is the appropriate s-shell form factor *normalized to unity* for $q=0$, in the limit of no absorption, ideal wave function matching, and ignoring recoil corrections.

In Tables VIII and IX we list the expressions for the reduced cross sections $(d\sigma/d\Omega_L)/\lvert N_{1s}^{(0)}(q)\rvert^2$ for ^{3}He and ^{4}He targets. A check on the correctness of these tables is provided by the sum over I and S of entries for $(\bar{p},p)$, which yields Z times the expression (A3) for one proton. In the case of $(\bar{p},n)$, each such sum gives Z times (A4) plus N times (A5). To establish contact with the general expression (4.1) of the main text, we note that α_{fi} is explicitly determined by the entries of Tables VIII and IX for s-shell targets. Thus, for the $^3\mathrm{He}(\bar{p},p)X$ process to the possibly narrow $S_x=\frac{3}{2}$ state, we obtain from Table VIII,

$$\alpha_{fi}=\frac{8\,\lvert b_{\sigma\tau}\rvert^2+16\,\lvert b_\tau^{TQ}\rvert^2}{4\,\lvert b_\tau\rvert^2+12\,\lvert b_{\sigma\tau}\rvert^2+24\,\lvert b_\tau^{TQ}\rvert^2}\,, \tag{A20}$$

where we divided the appropriate entry of the table by two since in the general formulation (4.1) this number of target protons belongs to the form factor.

As another example, we list in Table X the cross section expressions for $^{16}O(\bar{p},p)$ due to transitions of the type $1p_{3/2}\rightarrow np_j$. These results are appropriate for a ^{12}C target as well, if the latter is described by a closed $p_{3/2}$ shell. We implicitly assume here that the final $^{16}_{\bar{p}}C$ states are well described by specific j values. While this assumption may break down, for example, due to a $\bar{p}$-nuclear spin-orbit splitting comparable to that of a proton (6 MeV), it is adopted here for the sake of definiteness. The form factors $N_{1p}^{(\Delta L)}$ are defined in Ref. 25 [Eq. (3.13) of Auerbach *et al.*]. In the plane wave approximation they reduce to

$$N_{1p}^{(\Delta L)}=\int u_{1p}^{\bar{p}}(r)j_{\Delta L}\left[\left(\frac{A-1}{A}\right)qr\right]u_{1p}^{p}(r)dr\,. \tag{A21}$$

The α_{fi} coefficients of Eq. (4.1) can be readily read from the entries of Table X. Thus, at 0° where the $\Delta L=0$ transitions peak and dominate over the $\Delta L=2$ transitions, we have

$$\begin{aligned}\alpha_{fi}&=\frac{\lvert b_\tau\rvert^2}{(\lvert b_\tau\rvert^2+3\,\lvert b_{\sigma\tau}\rvert^2+6\,\lvert b_\tau^{TQ}\rvert^2)}\,,\\&=\frac{5(\lvert b_{\sigma\tau}\rvert^2+2\,\lvert b_\tau^{TQ}\rvert^2)}{3(\lvert b_\tau\rvert^2+3\,\lvert b_{\sigma\tau}\rvert^2+6\,\lvert b_\tau^{TQ}\rvert^2)}\,,\\&=\frac{4(\lvert b_{\sigma\tau}\rvert^2+2\,\lvert b_\tau^{TQ}\rvert^2)}{3(\lvert b_\tau\rvert^2+3\,\lvert b_{\sigma\tau}\rvert^2+6\,\lvert b_\tau^{TQ}\rvert^2)}\,,\end{aligned} \tag{A22}$$

for 0^-, $1^-(p_{3/2})$, and $1^-(p_{1/2})$, respectively. The sum of these coefficients is, of course, one. Note that the spin dependence enters here through the combination $(\lvert b_{\sigma\tau}\rvert^2+2\,\lvert b_\tau^{TQ}\rvert^2)$ as it did in Tables VIII and IX for

the $\Delta L=0$ transitions. This is not the case for the $\Delta L=2$ transitions in Table X for which orbital and spin contributions mix in a nontrivial way. However, when the cross sections of the table are summed up, the natural sum rule

$$\sum(d\sigma/d\Omega)(p_{3/2}\to p_j)=4(|b_\tau|^2+3|b_{\sigma\tau}|^2+6|b_\tau^{TQ}|^2)\times 4(|N_{1p}^{(0)}|^2+2|N_{1p}^{(2)}|^2) \quad \text{(A23)}$$

is satisfied.

*Present address: Theory Group, SIN, CH-5234 Villigen, Switzerland.

[1]D. Garreta *et al.*, Phys Lett. **135B**, 266 (1984); **139B**, 464 (1984); **149B**, 64 (1984); CERN Report CERN-EP/84-114, 1984.

[2]K. Nakamura *et al.*, Phys. Rev. Lett. **52**, 731 (1984); Tokyo report UT-HE-84/07, 1984.

[3]V. Ashford *et al.*, Phys. Rev. C **30**, 1080 (1984).

[4]D. Garreta *et al.*, Phys. Lett. **150B**, 95 (1985).

[5]N. DiGiacomo, private communication; J. W. Sunier *et al*, *Antiproton 1984. Proceedings of the VIIth European Symposium on Antiproton Interactions, Durham, England, 1984* (Hilger, London, 1985), p. 195—200.

[6]A. M. Green and S. Wycech, Nucl. Phys. **A377**, 441 (1982).

[7]A. M. Green, W. Stepien-Rudzka, and S. Wycech, Nucl. Phys. **A399**, 307 (1983).

[8]W. R. Gibbs and W. B. Kaufmann, Phys. Lett. **145B**, 1 (1984).

[9]J. Coté *et al.*, Phys. Rev. Lett. **48**, 1319 (1982).

[10]C. B. Dover and A. Gal, Phys. Lett. **110B**, 433 (1982).

[11]P. D. Barnes *et al.*, Phys. Rev. Lett. **29**, 1132 (1972).

[12]P. Roberson *et al.*, Phys. Rev. C **16**, 1945 (1977).

[13]H. Poth *et al.*, Nucl. Phys. **A294**, 435 (1978).

[14]C. J. Batty, Nucl. Phys. **A372**, 433 (1981).

[15]C. J. Batty, E. Friedman, and J. Lichtenstadt, Phys. Lett. **142B**, 241 (1984); Nucl. Phys. **A436**, 621 (1985).

[16]E. Friedman, private communication.

[17]J. Niskanen and A. M. Green, Nucl. Phys. **A404**, 495 (1983).

[18]H. V. von Geramb, K. Nakano, and L. Rikus, Lett. Nuovo Cimento **42**, 209 (1985).

[19]J. Kronenfeld, A. Gal, and J. M. Eisenberg, Nucl. Phys. **A430**, 525 (1984).

[20]A. J. Baltz, C. B. Dover, and M. E. Sainio, Bull. Am. Phys. Soc. **28**, 659 (1983); in *Proceedings of the International Conference on Nuclear Physics, Florence, Italy, 1983* (Tipografia Compositori, Bologna, Italy, 1983), Vol. 1, p. 388.

[21]C. J. Batty, Phys. Lett. **87B**, 324 (1979).

[22]C. Y. Wong, A. K. Kerman, G. R. Satchler, and A. D. MacKellar, Phys. Rev. C **29**, 574 (1984).

[23]J. H. Koch and M. M. Sternheim, Phys. Rev. Lett. **28**, 1061 (1972); we would like to thank Prof. Sternheim for supplying us with a copy of the code EXOTIC, a modified version of which was used here to obtain the complex eigenvalues of the optical potential.

[24]A. Gal, G. Toker, and Y. Alexander, Ann. Phys. (N.Y) **137**, 341 (1981).

[25]The coupled channels code CHUCK, supplied to us by P. D. Kunz, was used for our distorted wave calculations. The code was utilized with no back coupling, a mode which is equivalent to DWBA. The form factor $F_{fi}(q)$ includes recoil corrections ignored in the schematic form (4.2). More details may be found in the analysis of (K^-,π) reactions by E. H. Auerbach *et al.*, Ann. Phys. (N.Y.) **148**, 381 (1983).

[26]C. Rolland *et al.*, Nucl. Phys. **80**, 625 (1966).

[27]M. Alston-Garnjost *et al.*, Phys. Rev. Lett. **43**, 1901 (1979).

[28]H. Heiselberg, A. S. Jensen, A. Miranda, and G. C. Oades, Phys. Lett. **132B**, 279 (1983).

[29]M. Cahay, J. Cugnon, and J. Vandermeulen, Nucl. Phys. **A393**, 237 (1983).

[30]M. R. Clover, R. M. DeVries, N. J. DiGiacomo, and Y. Yariv, Phys. Rev. C **26**, 2138 (1982).

[31]A. S. Iljinov, V. I. Nazaruk and S. E. Chigrinov, Nucl. Phys. **A382**, 378 (1982).

[32]A. Gal and C. B. Dover, Phys. Rev. Lett. **44**, 379 (1980); **44**, 962(E) (1980).

[33]P. H. Timmers, W. A. van der Sanden, and J. J. de Swart, Phys. Rev. D **29**, 1928 (1984).

[34]M. Maruyama and T. Ueda, Nucl. Phys. **A364**, 297 (1981); Phys. Lett. **149B**, 436 (1984).

[35]A. M. Green and J. A. Niskanen, Nucl. Phys. **A412**, 448 (1984).

[36]C. B. Dover, Nucl. Phys. **A416**, 313c (1984); this paper reviews various models for the spin-isospin dependence of the $N\bar{N}$ absorptive potential.

[37]C. B. Dover and J. M. Richard, Phys. Rev. C **21**, 1466 (1980).

[38]M. Lacombe, B. Loiseau, B. Moussallam, and R. Vinh Mau, Phys. Rev. C **29**, 1800 (1984).

[39]L. Gray, P. Hagerty, and T. E. Kalogeropoulos, Phys. Rev. Lett. **26**, 1491 (1971).

[40]W. G. Love and M. A. Franey, Phys. Rev. C **24**, 1073 (1981); **27**, 438(E) (1983).

[41]C. B. Dover, M. E. Sainio, and G. E. Walker, Phys. Rev. C **28**, 2368 (1983).

[42]O. D. Dalkarov, B. O., Kerbikov, I. A. Rumyantsev, and I. S. Shapiro, Yad. Fiz. **17**, 1321 (1973) [Sov. J. Nucl. Phys. **17**, 688 (1973)].

[43]C. B. Dover and A. Gal, Ann. Phys. (N.Y.) **146**, 309 (1983).